Charged hadron production in central Xe+La collisions at the CERN SPS

Oleksandra Panova

Jan Kochanowski University of Kielce
NA61/SHINE collaboration, CERN

December 7, 2022

1. Introduction
   - Kaon/pion ratio and the onset of deconfinement
   - Protons and the onset of deconfinement
2. NA61/SHINE experiment
3. $\mathrm{d}E/\mathrm{d}x$ method for charged hadrons identification
4. h^- method for π^- identification
5. Summary and further plans

Research goals

The main goal:

Obtain spectra of charged hadrons produced in Xe+La interactions at six beam momenta in the range of $13A$–$150A$ GeV/c.

Obtained spectra will allow to investigate horn and proton rapidity spectra shape as a signature of the onset of deconfinement.

The project is an **important part of the NA61/SHINE** 2D scan in collision energy and system size.

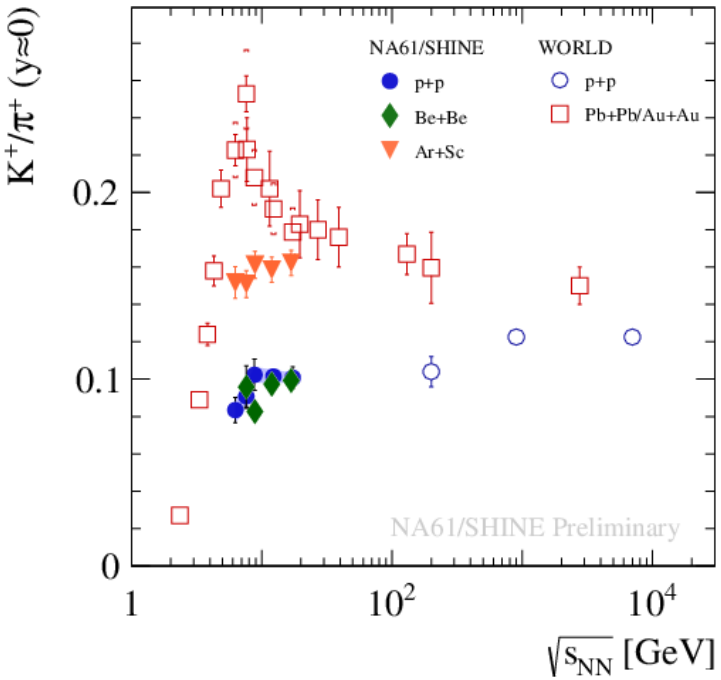

Phases of strongly interacting matter

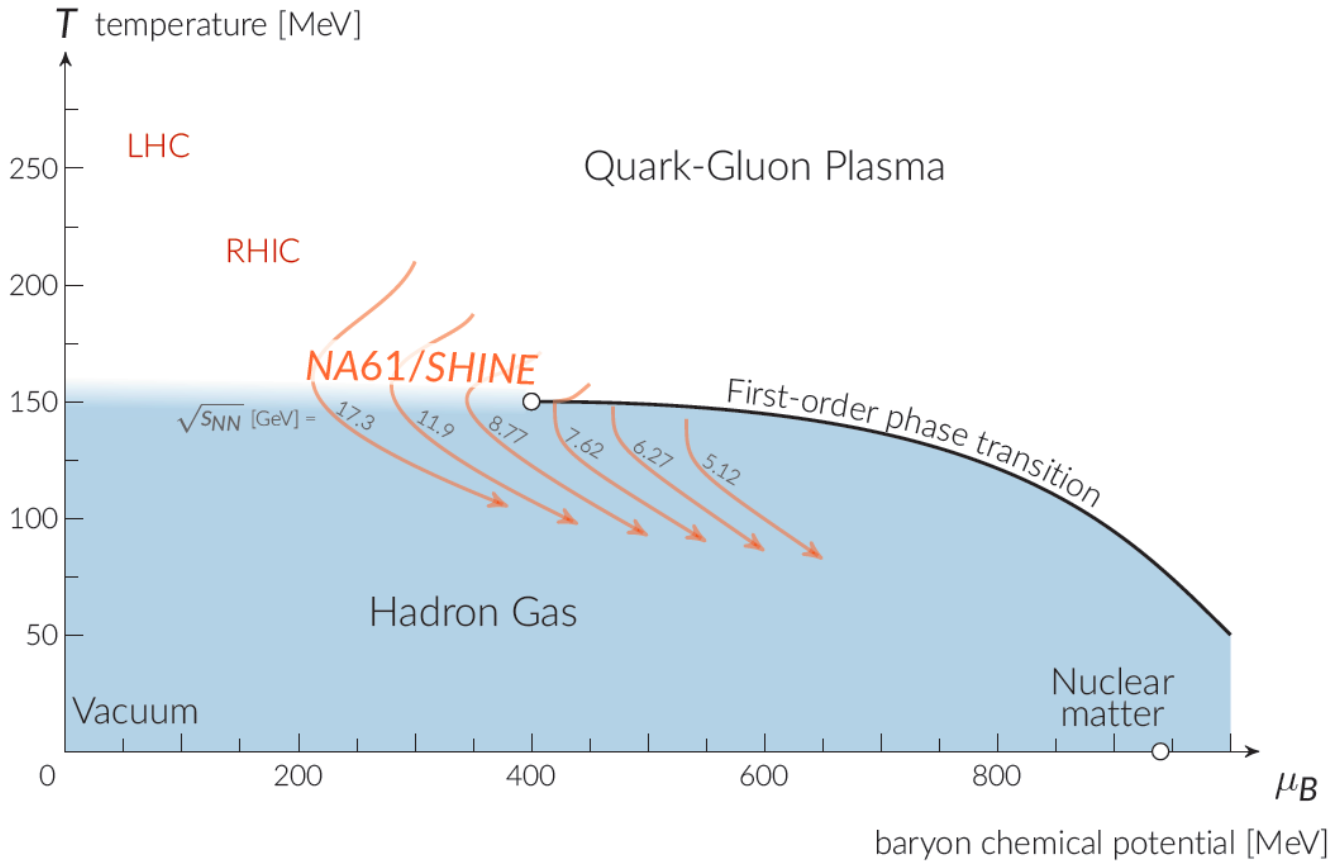

Signatures of the onset of deconfinement

$F \approx (\sqrt{s_{NN}})^{1/2}$

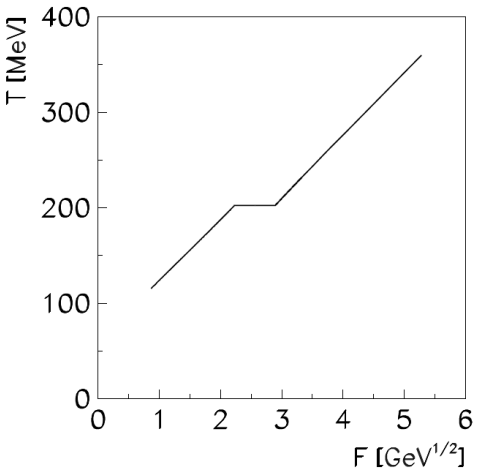

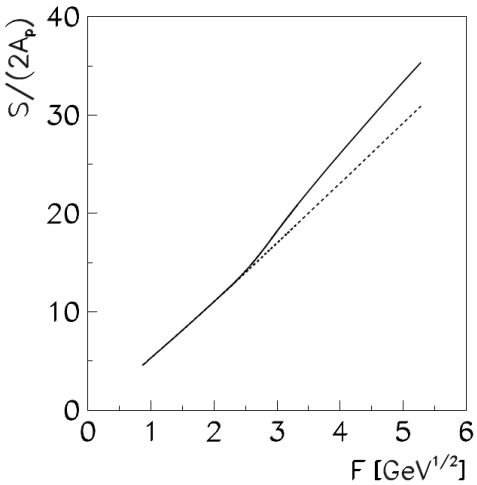

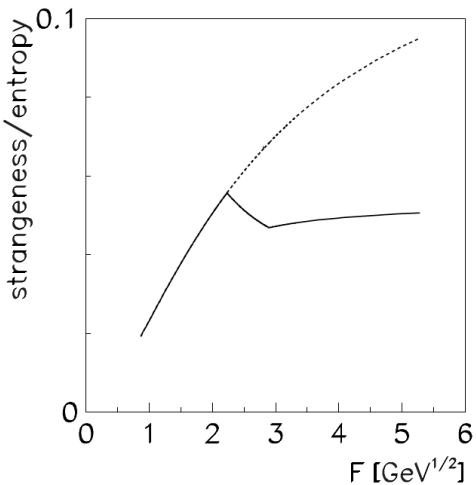

Step Kink Horn

M. Gaździcki, M.I. Gorenstein, On the Early Stage of Nucleus–Nucleus Collisions Acta Phys. Pol. B 30, 2705 (1999)

Signatures of the onset of deconfinement: horn

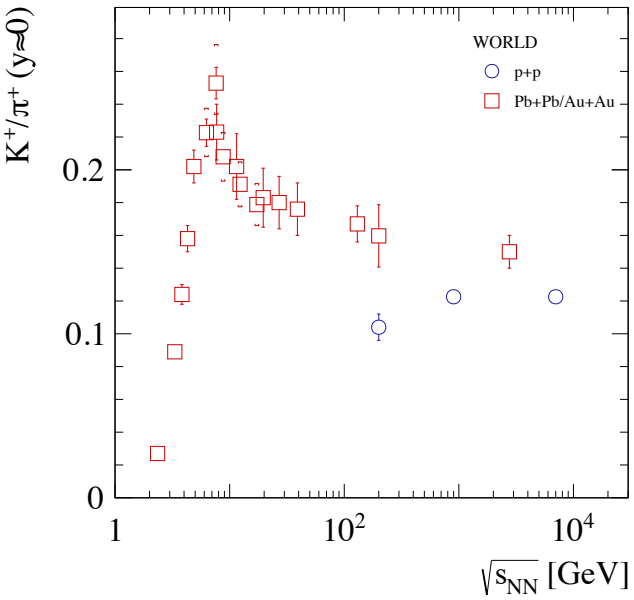

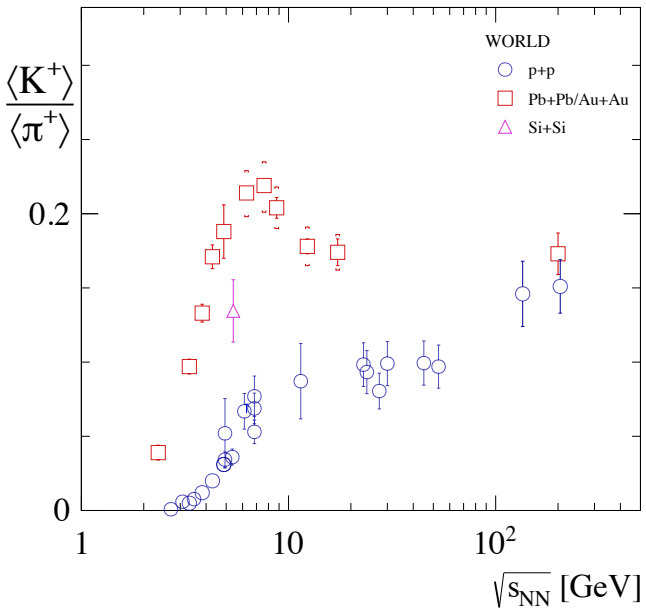

$\langle K^+/\pi^+ \rangle$ ratio at mid-rapidity (left plot) and in whole phase space "4π" (on the right) in dependence on collision energy $\sqrt{s_{NN}}$

Signatures of the onset of deconfinement: horn

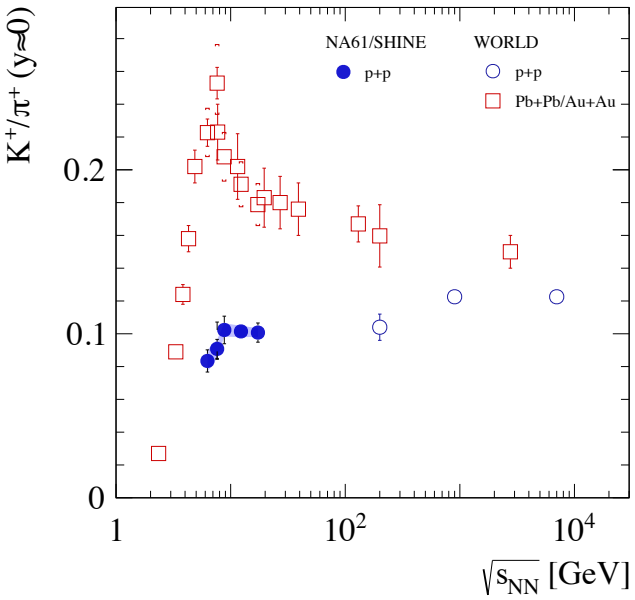

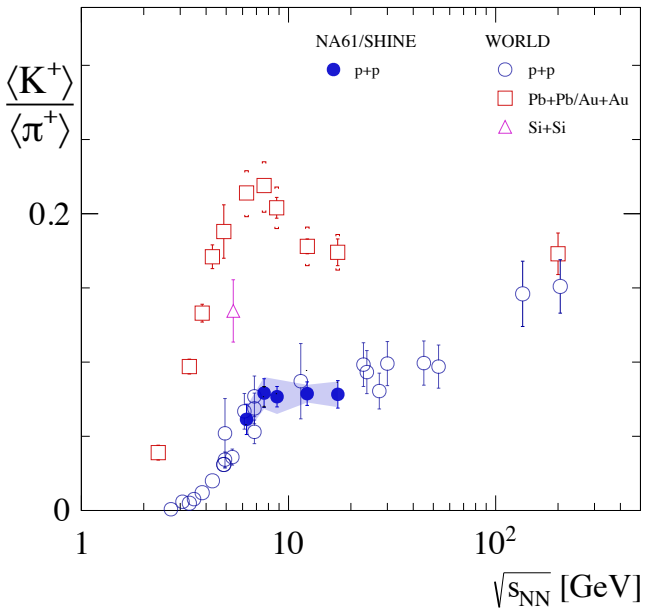

$\langle K^+/\pi^+ \rangle$ ratio at mid-rapidity (left plot) and in whole phase space "4π" (on the right) in dependence on collision energy $\sqrt{s_{NN}}$

NA61/SHINE data:

p+p: Eur. Phys. J. C 77.10 (2017), p. 671, Eur. Phys. J. C 74.3 (2014), p. 2794.

Signatures of the onset of deconfinement: horn

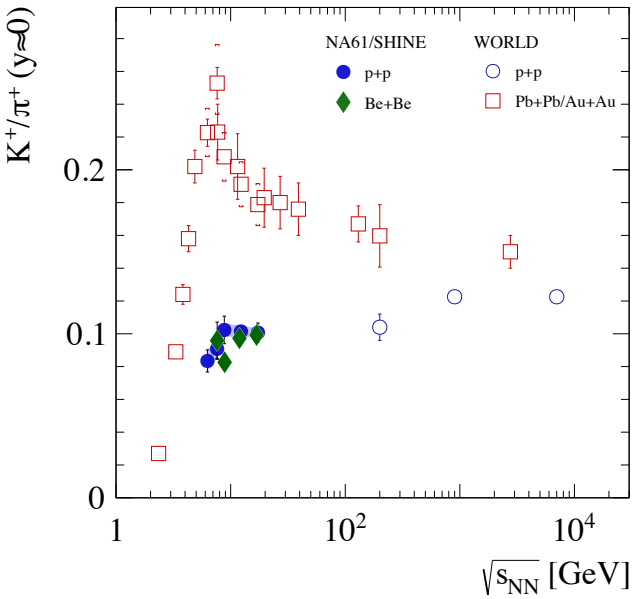

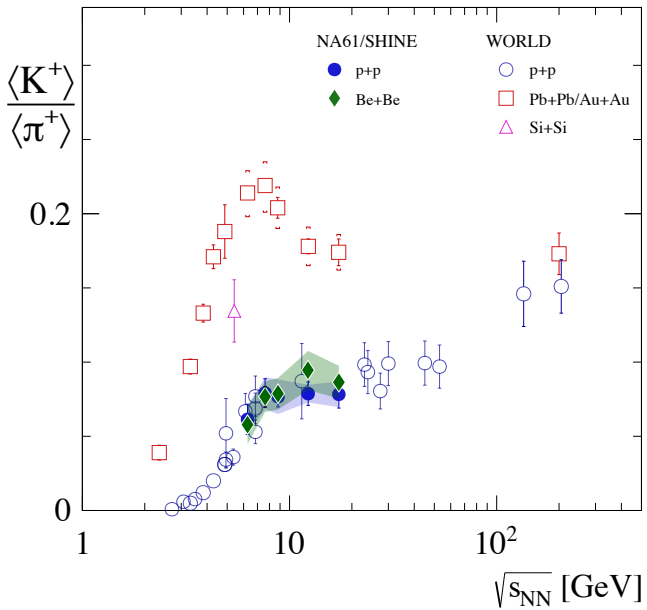

$\langle K^+/\pi^+ \rangle$ ratio at mid-rapidity (left plot) and in whole phase space "4π" (on the right) in dependence on collision energy $\sqrt{s_{NN}}$

NA61/SHINE data:
p+p: Eur. Phys. J. C 77.10 (2017), p. 671, Eur. Phys. J. C 74.3 (2014), p. 2794.
^{7}Be+^{9}Be: Phys. J. C 80.10 (2020), p. 961, Eur. Phys. J. C 81.1 (2021), p. 73.

Signatures of the onset of deconfinement: horn

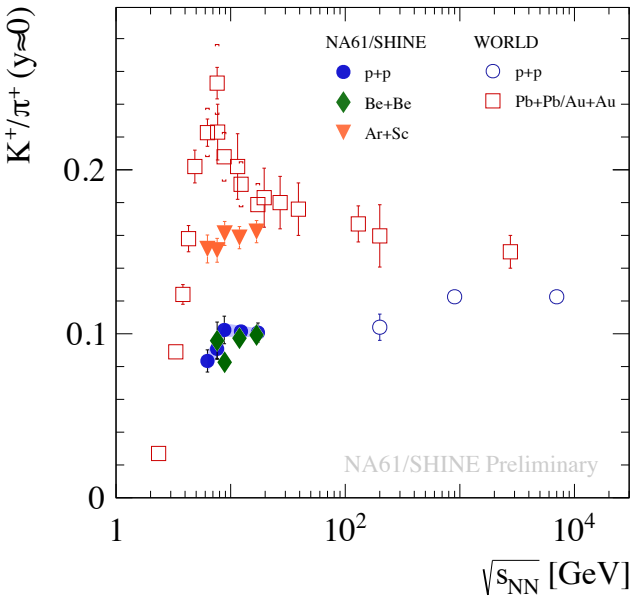

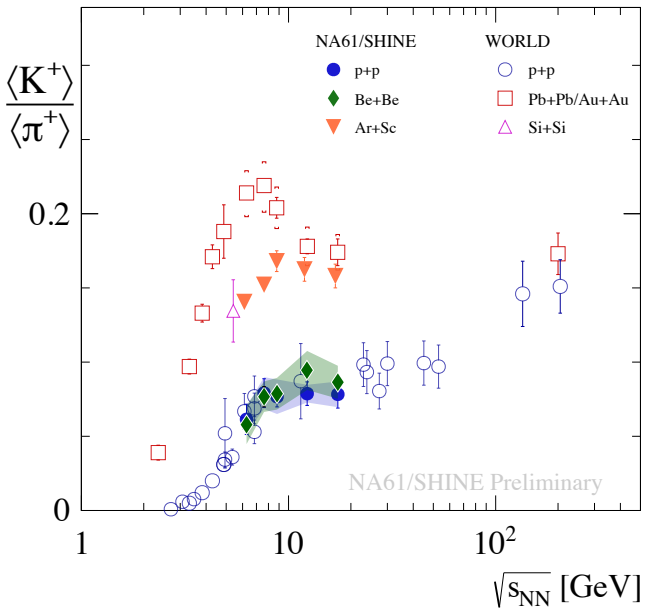

$\langle K^+/\pi^+ \rangle$ ratio at mid-rapidity (left plot) and in whole phase space "4π" (on the right) in dependence on collision energy $\sqrt{s_{NN}}$

NA61/SHINE data:

p+p: Eur. Phys. J. C 77.10 (2017), p. 671, Eur. Phys. J. C 74.3 (2014), p. 2794.

^{7}Be+^{9}Be: Phys. J. C 80.10 (2020), p. 961, Eur. Phys. J. C 81.1 (2021), p. 73.

^{40}Ar+^{45}Sc: Eur. Phys. J. C 81.5 (2021), p. 397.

Protons and the onset of deconfinement

Protons at SPS energies:

- relatively abundant among products of nuclear collisions,
- relatively easy to identify (mass is significantly larger than π and K masses),
- rapidity distributions are weakly affected by processes at the final stages of collisions,
- **rapidity distributions were suggested to be sensitive to the onset of deconfinement.**

Ivanov, PLB 690 (2010) 358

“Peak-dip-peak-dip” irregularity in p rapidity spectra

Reason of irregularity – onset of deconfinement!

For the EoS with a phase transition:

$\sqrt{s_{NN}}_1$ < $\sqrt{s_{NN}}_2$ < $\sqrt{s_{NN}}_3$ < $\sqrt{s_{NN}}_4$

peak dip peak dip

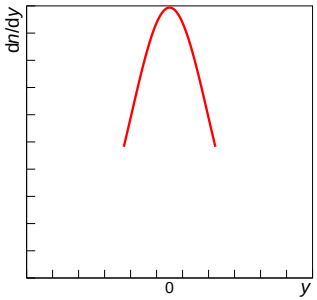

stiff EoS – spherical fireball

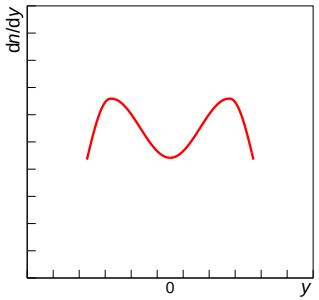

softest point region of the EoS – deformed fireball

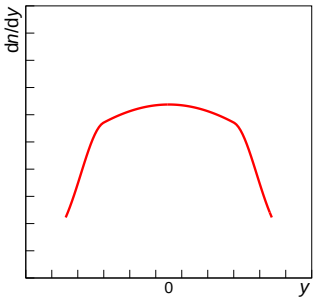

stiffness of the EoS grows – less deformed fireball

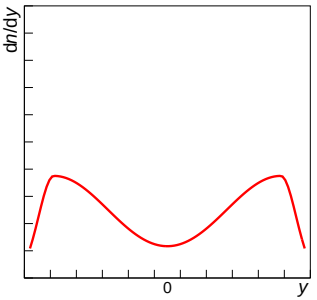

kinetic pressure overcomes stiffness of the EoS – deformed fireball

Ivanov, Blaschke, EPJ A (2016) 52: 237

“Peak-dip-peak-dip” irregularity in p rapidity spectra

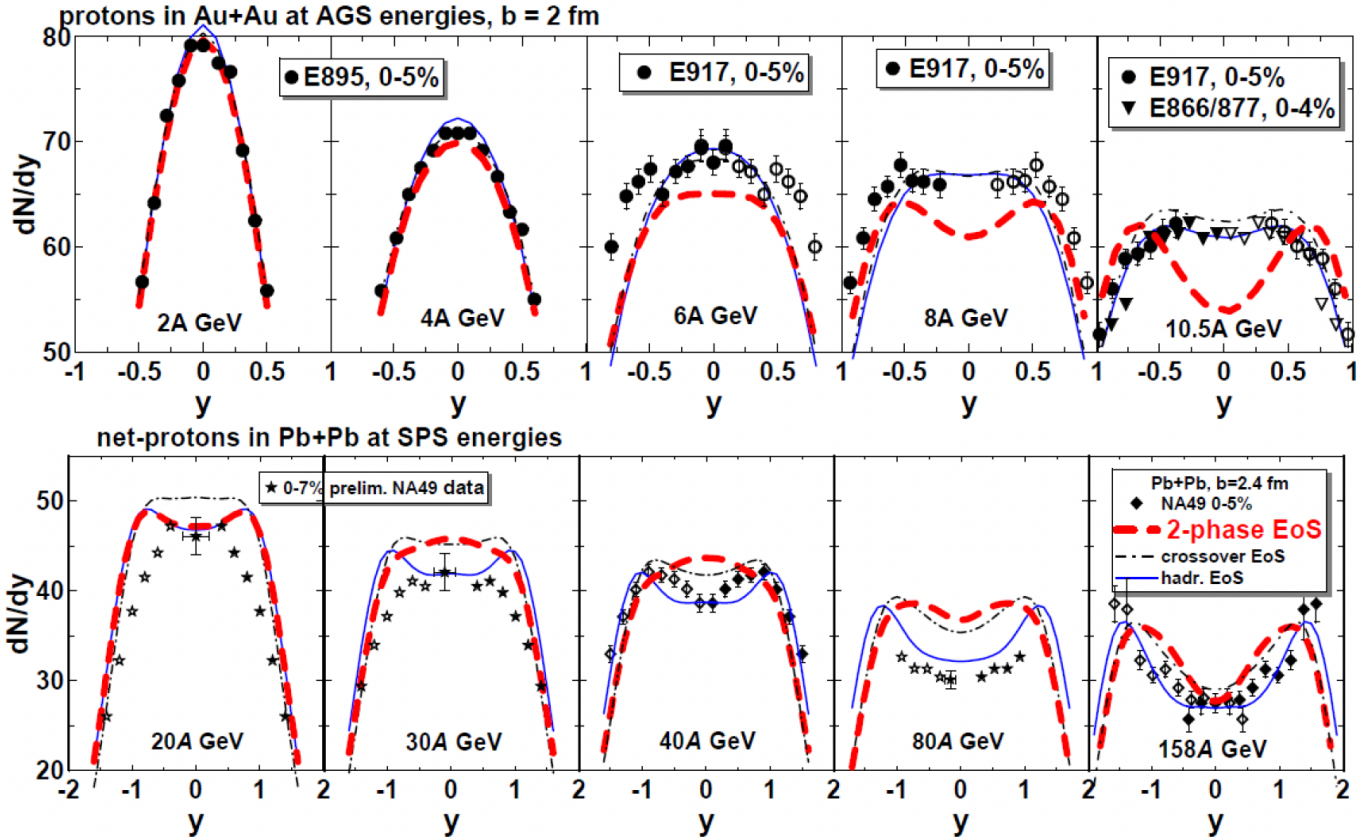

“Peak-dip-peak-dip” irregularity exists for Au+Au and Pb+Pb. Only 2-phase EoS model describes data qualitatively.

Ivanov, Blaschke, EPJ A (2016) 52: 237

NA61/SHINE 2D scan

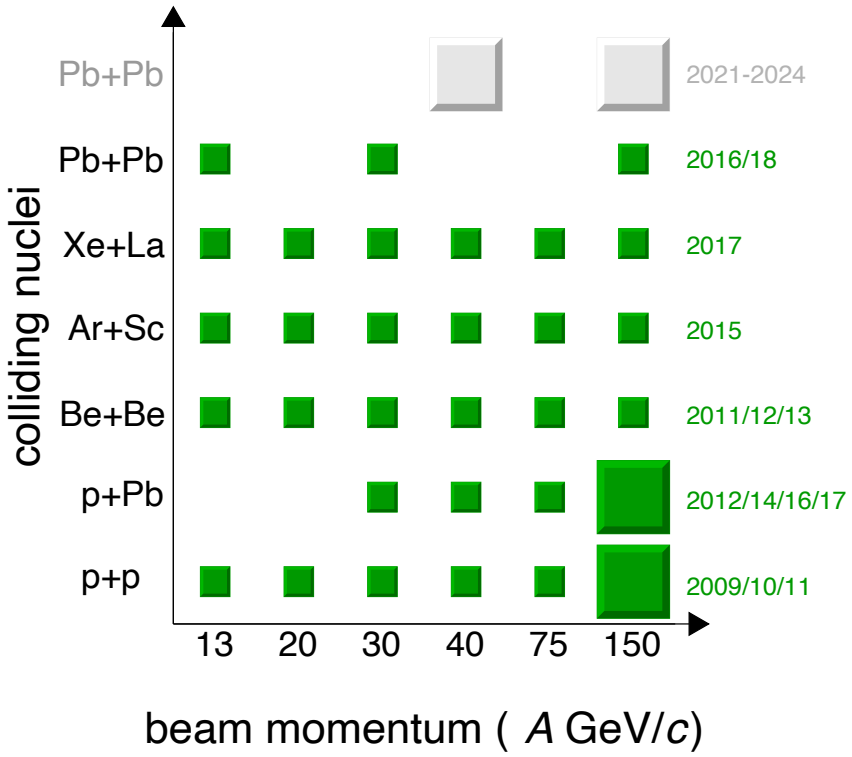

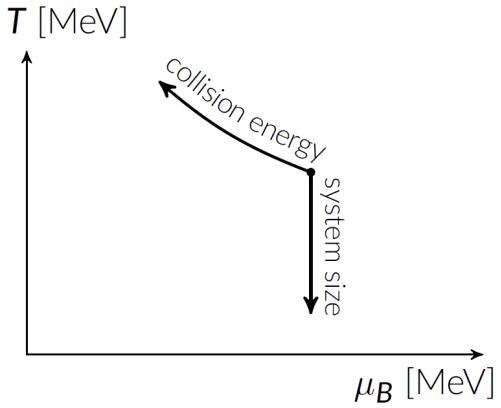

Becattini, Manninen, Gaździcki
Phys. Rev. C 73, 044905 (2006)

2D scan in collision energy and mass of the colliding nuclei.

NA61/SHINE 2D scan

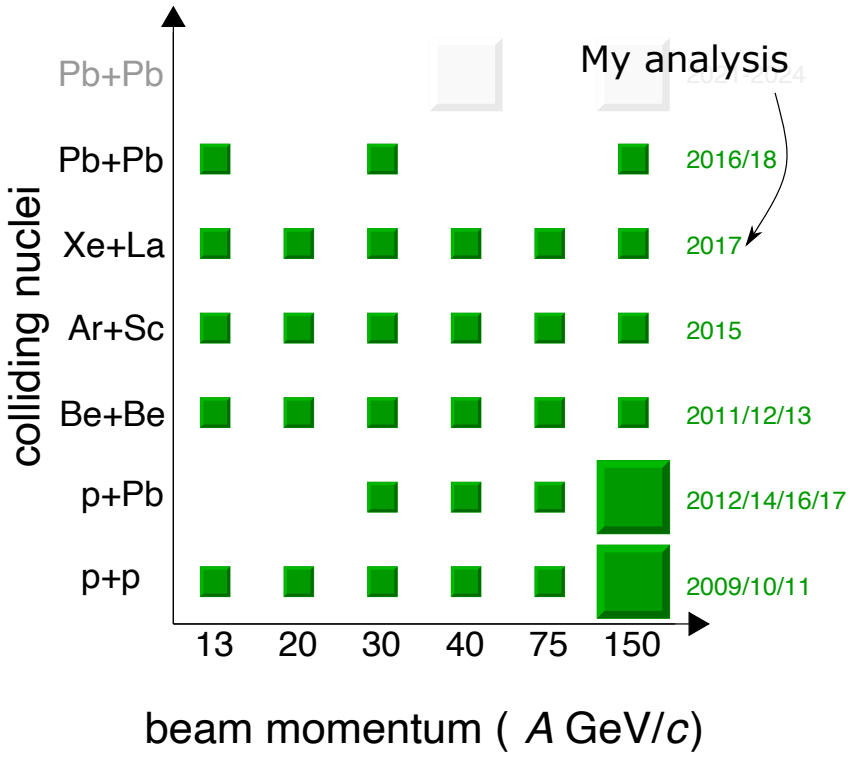

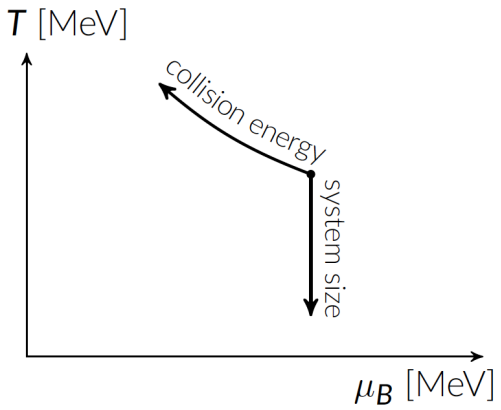

Becattini, Manninen, Gaździcki
Phys. Rev. C 73, 044905 (2006)

2D scan in collision energy and mass of the colliding nuclei.

NA61/SHINE experiment

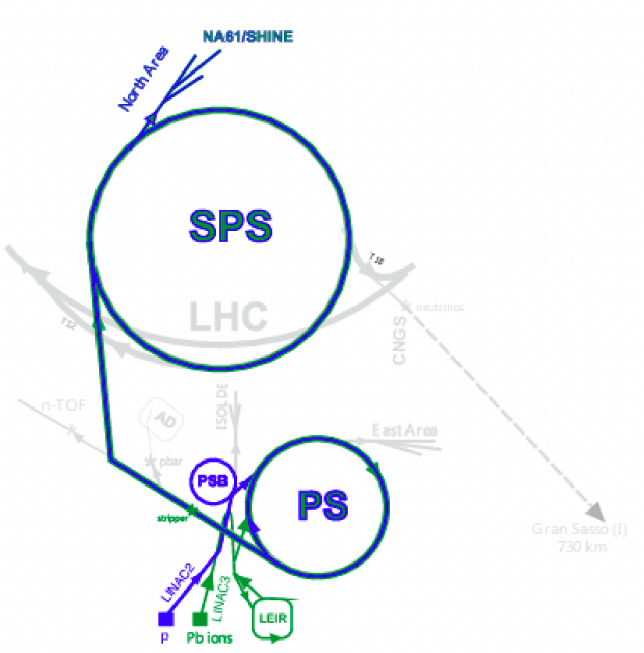

- Particle physics experiment at SPS at CERN.
- Fixed target.
- Two main physics goals:
  1. studies of proton–proton and nucleus–nucleus collisions to identify the **properties of the onset of deconfinement** and search of the critical point,
  2. neutrino and cosmic-ray studies (hadron–nucleus collisions).

Layout of the NA61/SHINE experimental setup

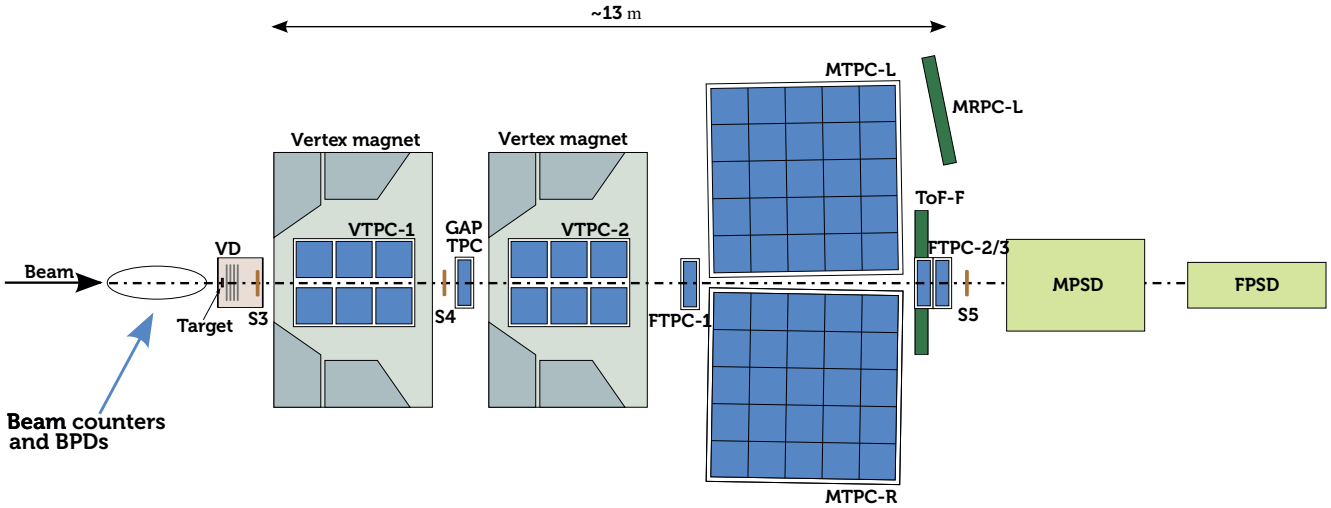

Large acceptance hadron spectrometer
– coverage of the full forward hemisphere, down to $p_T = 0.0$

^{129}Xe + ^{139}La collision at 150A GeV/c

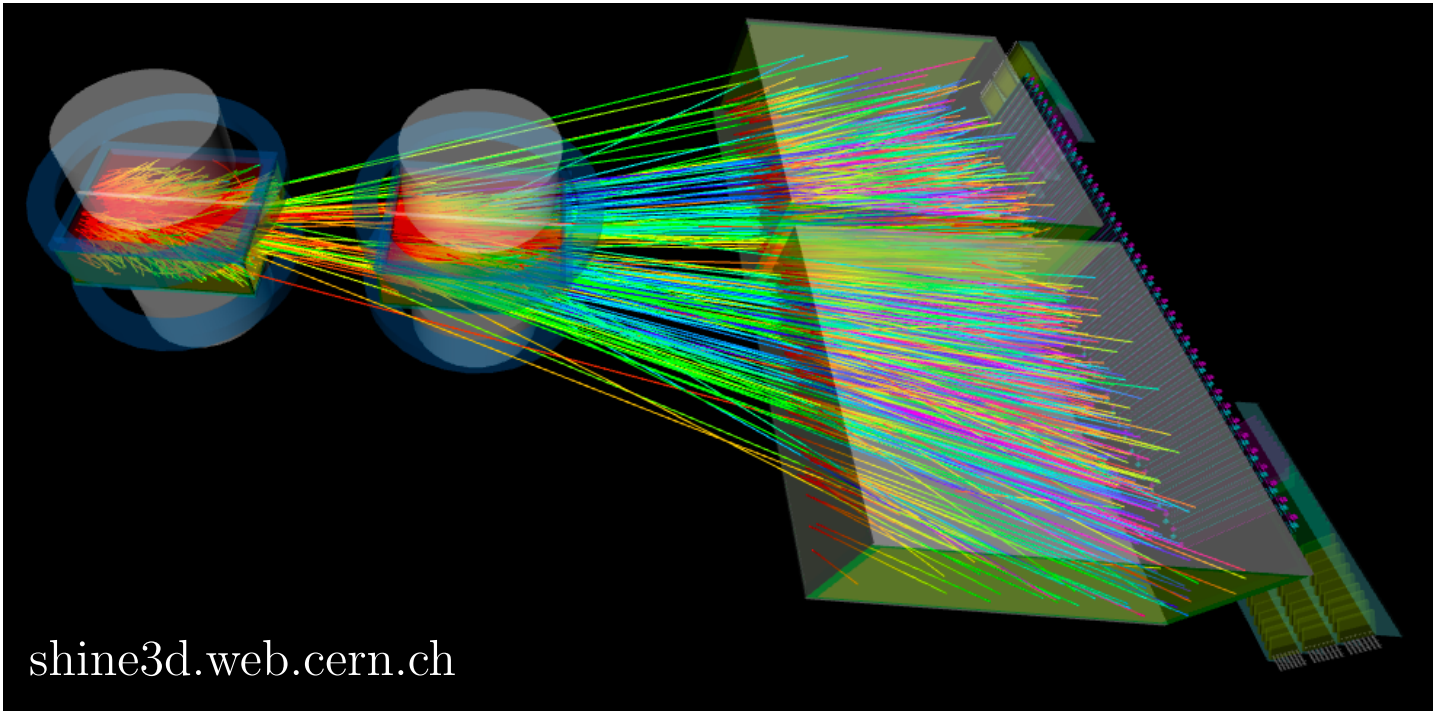

Maximum number of clusters:
72(VTPC1) + 72(VTPC2) + 90(MTPC) = 234

What can we measure in TPC?

- Charge – from the direction of deflection.
- Momentum – from the curvature of track:
  Transverse $p_{xz} = qBr$,
  Longitudinal $p_y = p_{xz}/\tan\theta$,
  θ – angle between $\vec{B}$ and $\vec{p}$.
- Energy loss.
- Track topology.

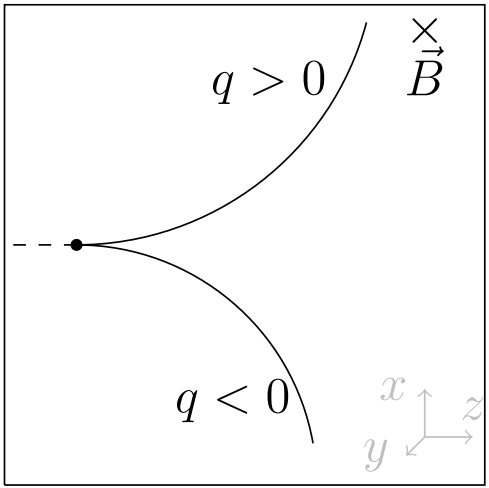

Data selection: Event cuts

Two types of cuts:

- upstream (not biasing):
  - only one beam particle,
  - well measured beam,
  - no detector malfunctioning.
- downstream (biasing):
  - 30% of the most central events,
  - main vertex present,
  - good quality of vertex fit,
  - fitted z-position of the main vertex is within 10 cm from the middle of the target.

Data selection: Vertex track cuts

- Tracks pointing to the main vertex,
- tracks with $q \cdot p_x > 0$,
- total number of measured clusters > 30 (maximum is 234),
- number of measured VTPC clusters > 15 (maximum is 144),
- ratio of measured clusters to potential points is within (0.5,1.1),
- azimutal angle $|\varphi| < 30°$ (only for $\mathrm{d}E/\mathrm{d}x$).

Methods of particle identification applied by me

- $\mathrm{d}E/\mathrm{d}x$:
  - Works for all relatively abundant charged particle with momenta $\gtrsim 5$ GeV/c.
  - Bethe equation allows to identify particle if its momentum and energy loss are known.
- h^-:
  - Works only for π^-.
  - Works for all momenta.
  - Idea: 90% of negative produced particles are pions, so we can measure pions using distribution of all negatively charged hadrons with MC corrections.

MC generated spectra

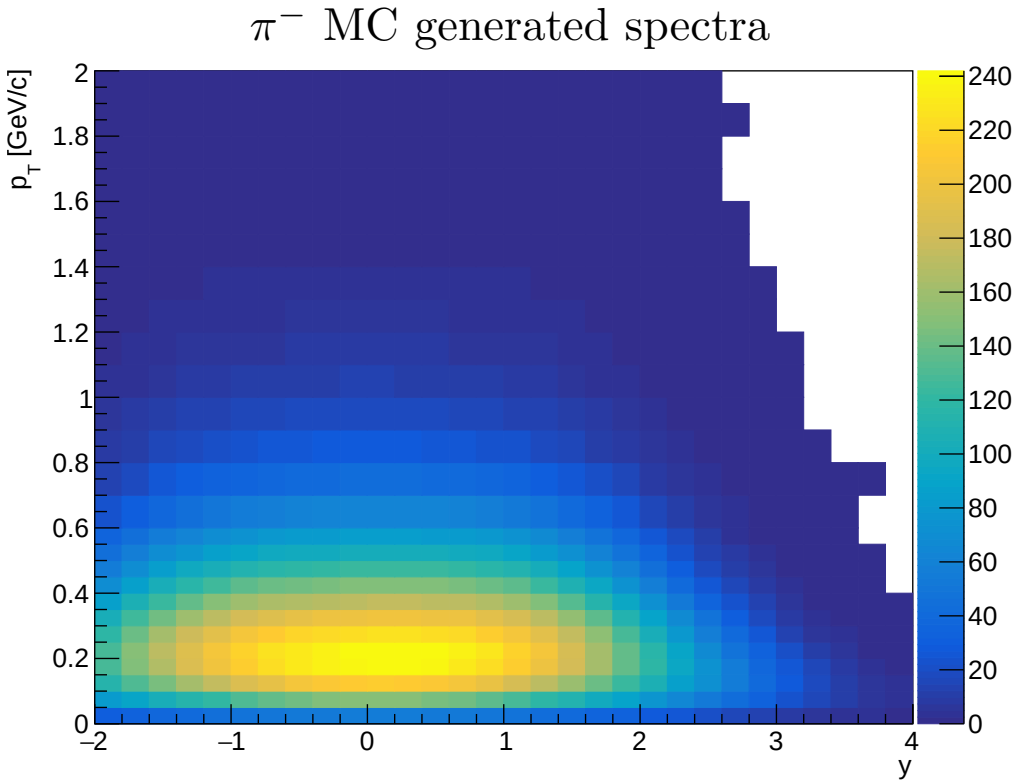

π^- spectrum simulated using MC –
real spectra of π^- should be the same.

Data reconstructed spectra

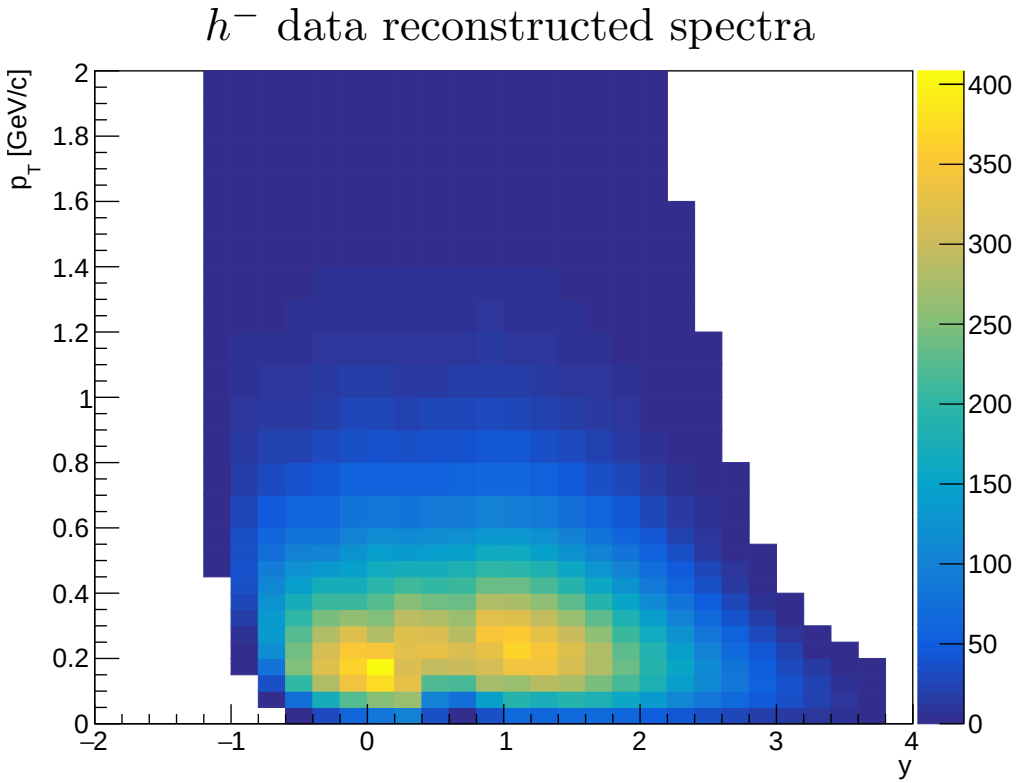

h^- spectrum measured by the detector – distorted spectra with limited acceptance.

Monte Carlo corrections

Why corrections are needed:

- Not full geometrical acceptance of the detector.
- Corrections for detector response, reconstruction efficiency.
- Corrections for contamination of vertex tracks with ones produced in secondary interactions.

Correction factor is calculated for each bin using formula:

$$n[i]_{\text{corr}} = n[i]_{\text{raw}} \times \frac{n[i]^{\text{MC}}_{\text{gen}}}{n[i]^{\text{MC}}_{\text{sel}}} \quad (\text{for } \mathrm{d}E/\mathrm{d}x),$$

$$n[i]^{\text{corrected}}_{\pi^-} = n[i]^{\text{raw data}}_{h^-} \times \frac{n[i]^{\text{MCgen}}_{\pi^-}}{n[i]^{\text{MCsel}}_{h^-}} \quad (\text{for } h^-).$$

$\mathrm{d}E/\mathrm{d}x$ vs p after all cuts

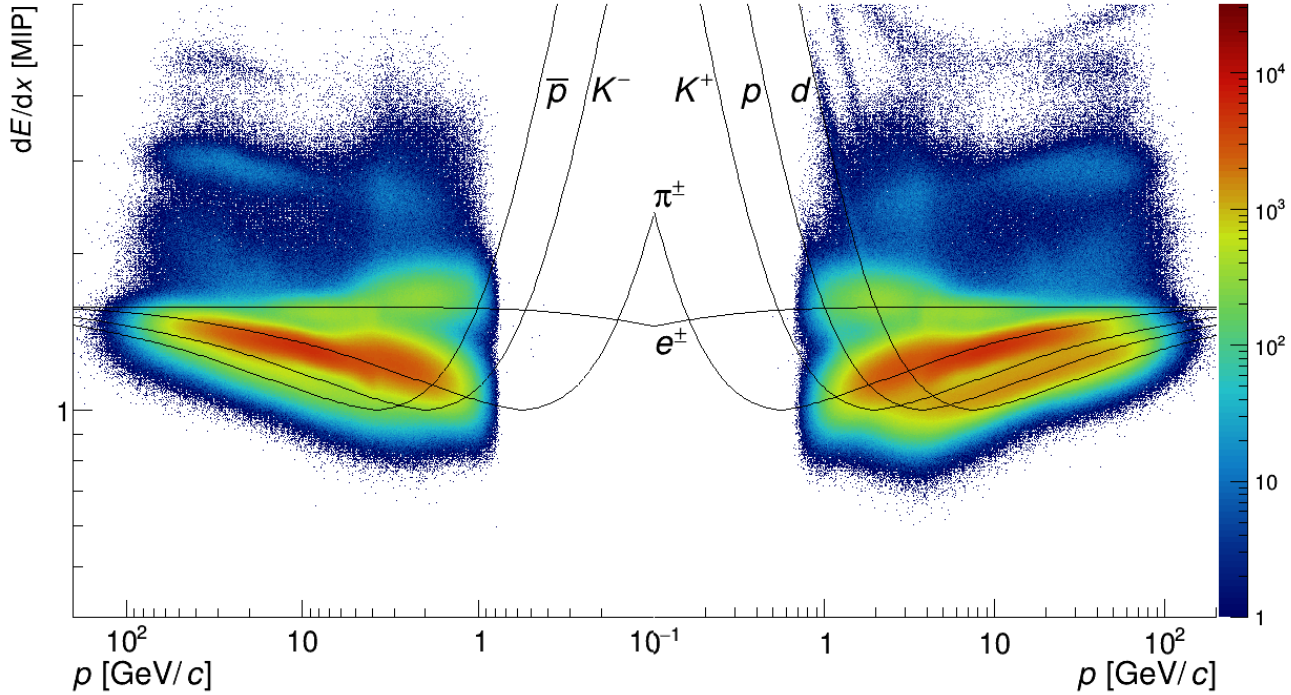

Bethe: $\left\langle -\frac{dE}{dx} \right\rangle = \frac{A}{\beta^2} \left[\ln B\beta^2\gamma^2 - 2\beta^2 - \delta(\beta\gamma) \right]$, $(0.1 \leq \beta\gamma \leq 1000)$

Fitting

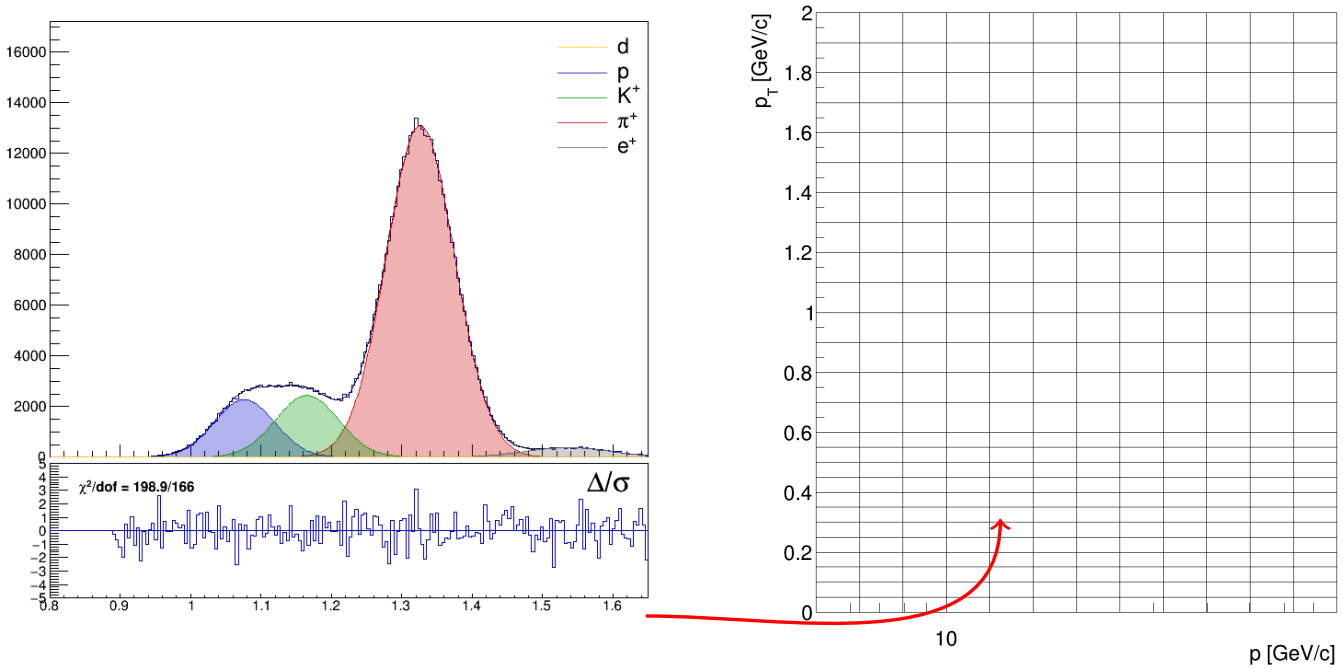

Fit with sum of asymmetric Gaussians for $p, \bar{p}, K^{\pm}, \pi^{\pm}, e^{\pm}, d$:

$$f(x) = \sum_{i=p,K,\pi,e,d} N_i \frac{1}{\sum_l n_l} \sum_l \frac{n_l}{\sqrt{2\pi}\sigma_{i,l}} \exp\left[-\frac{1}{2}\left(\frac{x - x'_i}{(1 \pm \delta)\sigma_{i,l}}\right)^2\right],$$

φ dependence

All φ

$-30^\circ < \varphi < 30^\circ$

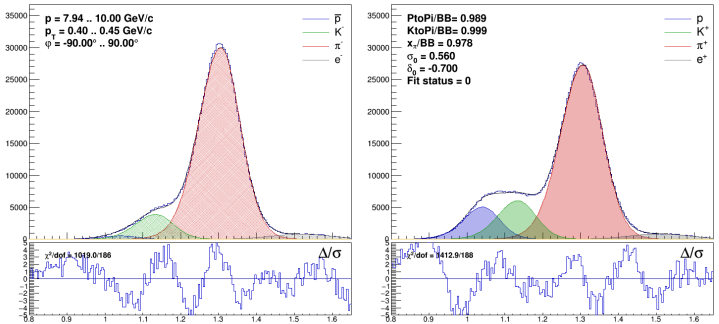

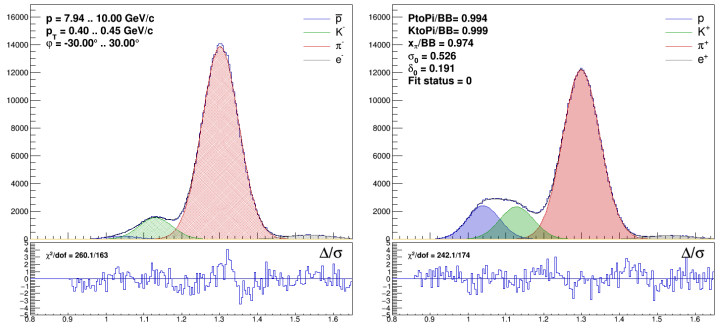

No local minimum between K and π peaks.

Local minimum between K and π peaks.

Significant improvement in resolution and quality of fit for $\varphi \in (-30^\circ, 30^\circ)$.

Raw spectra obtained using identity method

Negative:

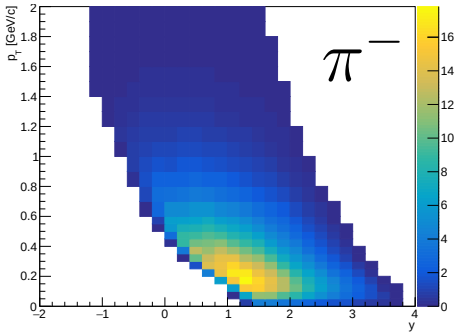

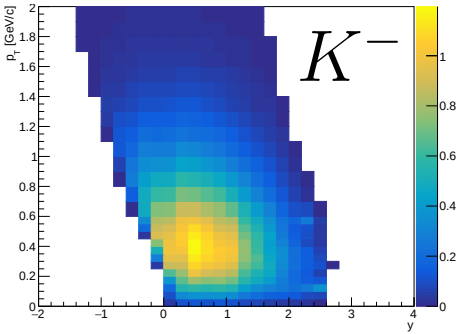

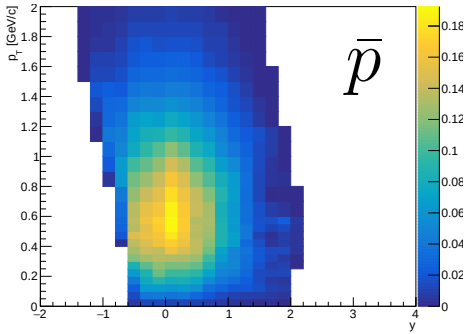

Positive:

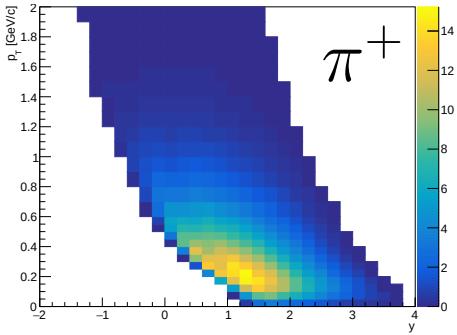

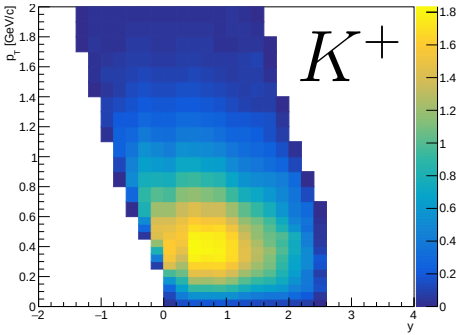

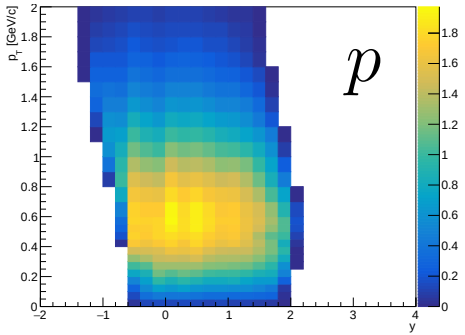

Corrected spectra

Negative:

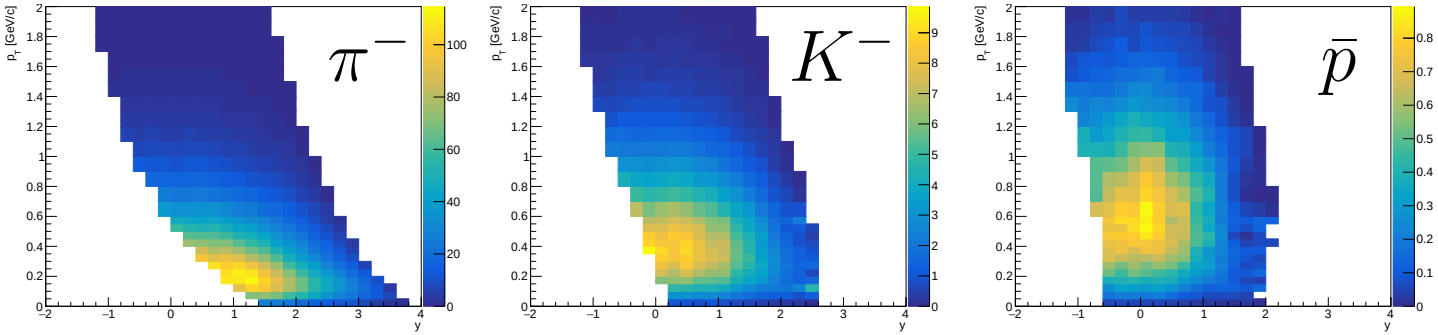

Positive:

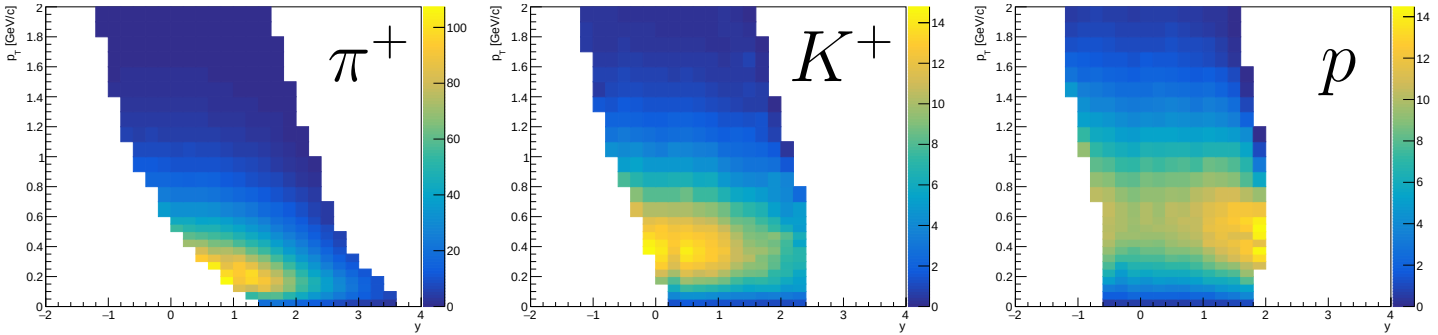

h^- method

h^- raw spectra

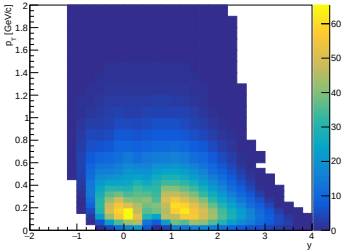

×

π^- MC gen

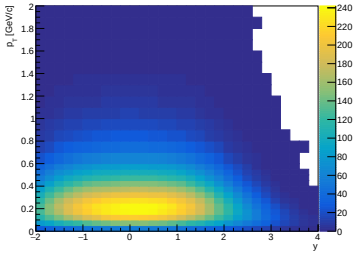

h^- MC sel

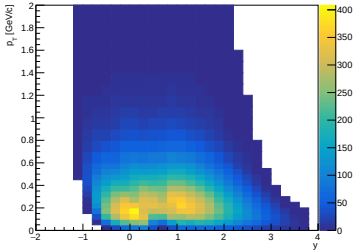

=

π^- corrected spectra

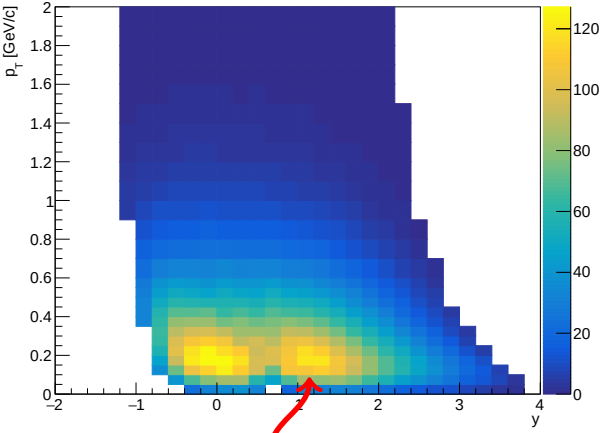

Problem! Not smooth distribution with "valley" at $y = 0.4 - 0.8$

π^- corrected spectra

Vertex track cuts: Track status, Impact parameter, RSTracks

+ all_clusters > 5

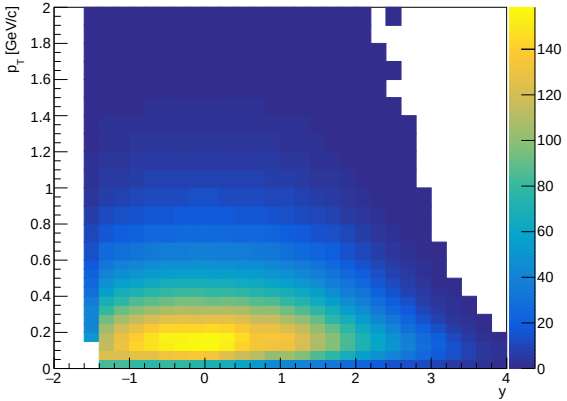

+ VTPC_clusters > 15

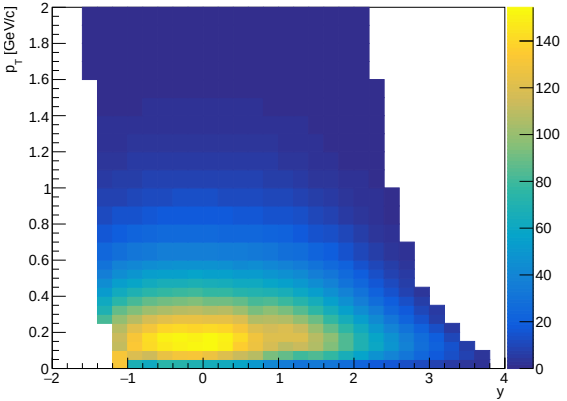

+ all_clusters > 30

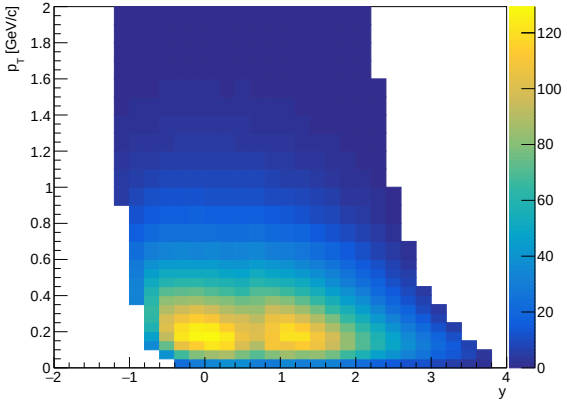

+ ratio cut

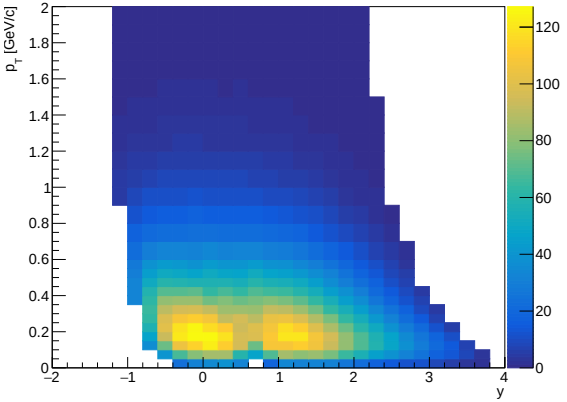

All clusters MC for Xe+La and Ar+Sc

Vertex track cuts:
Track status, Impact parameter, RSTracks, All clusters > 5

Xe+La

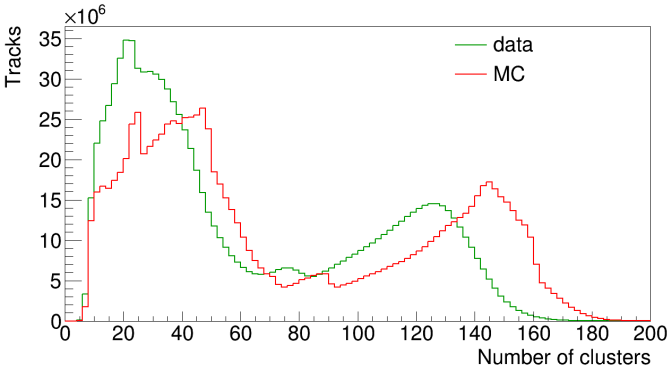

Ar+Sc

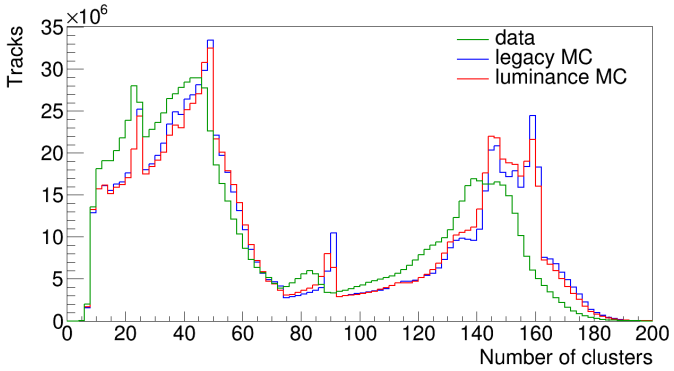

Ar+Sc is better described by MC than Xe+La.

Possible reasons for difference:

- Inefficient merging of track parts from different TPCs.
- Loss of clusters during reconstruction.

Clusters distributions

VTPC1 clusters

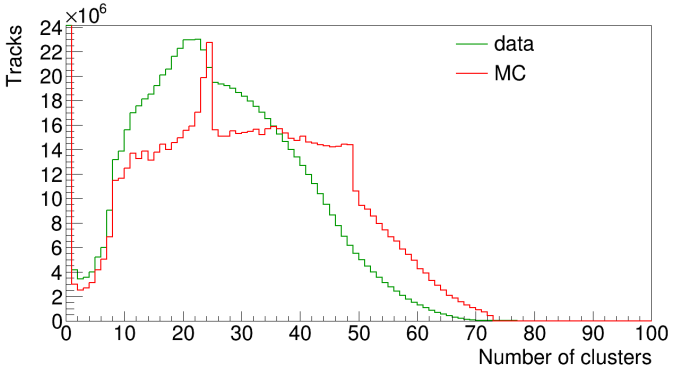

VTPC2 clusters

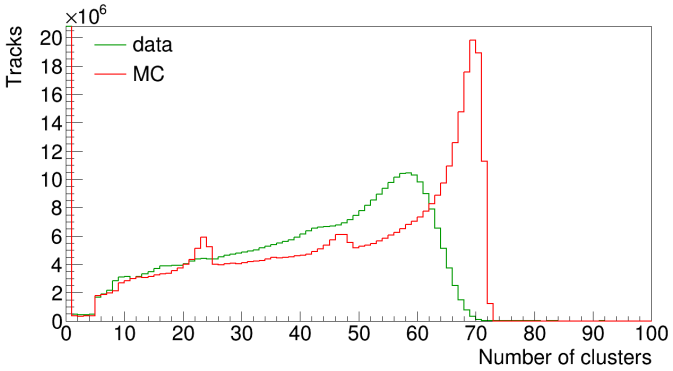

Vertex track cuts:
Track status, Impact parameter, RSTracks, All clusters > 5

MTPC clusters

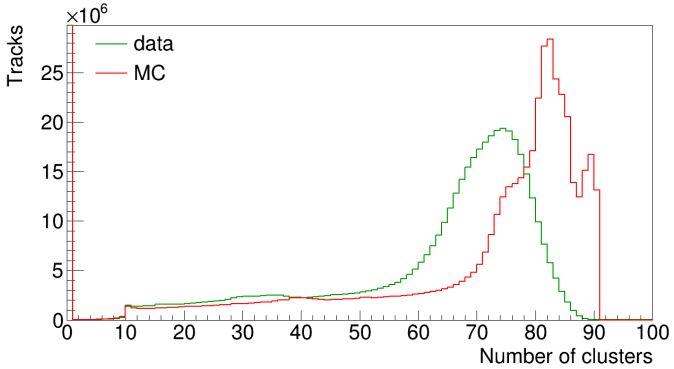

Data distributions are shifted and smeared comparing to MC.

Clusters distributions. Different multiplicities.

VTPC1 clusters

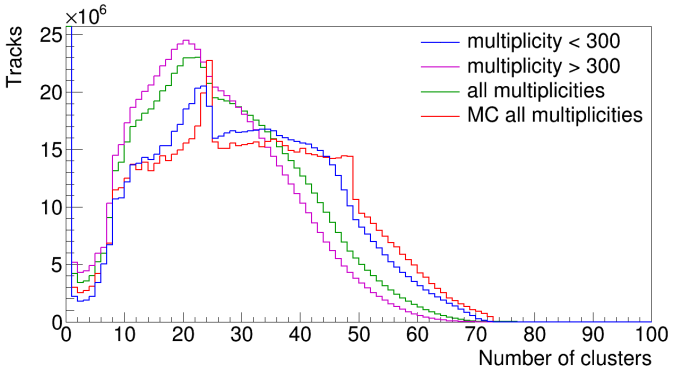

VTPC2 clusters

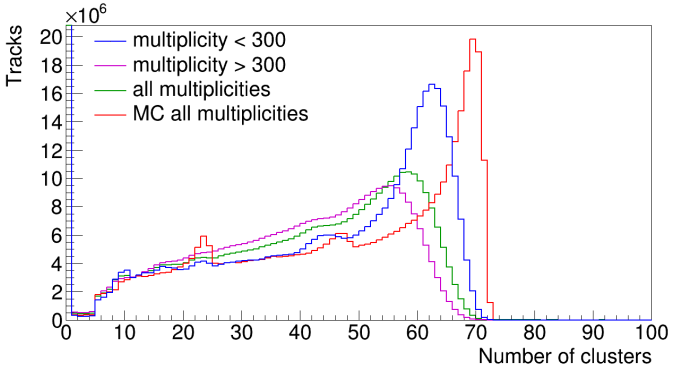

Vertex track cuts:
Track status, Impact parameter, RSTracks, All clusters > 5

MTPC clusters

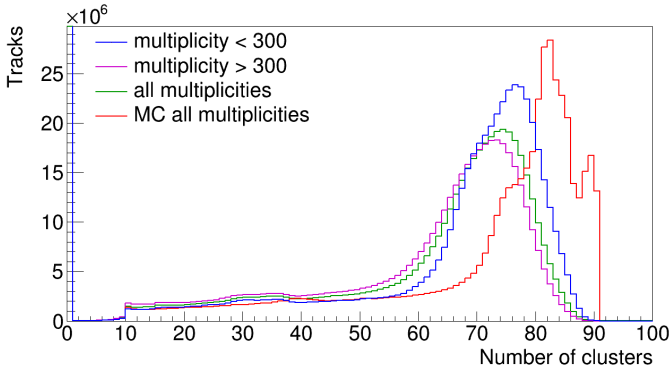

Cluster distribution for low multiplicity (< 300) events are closer to MC, than for high multiplicity (> 700).

Problem with high track density!

Clusters positions. $y = 0.4 - 0.8,\ p_T = 0.1 - 0.3$

Vertex track cuts: Track status, Impact parameter, RSTracks, All clusters > 30, VTPC clusters > 30, ratio cut

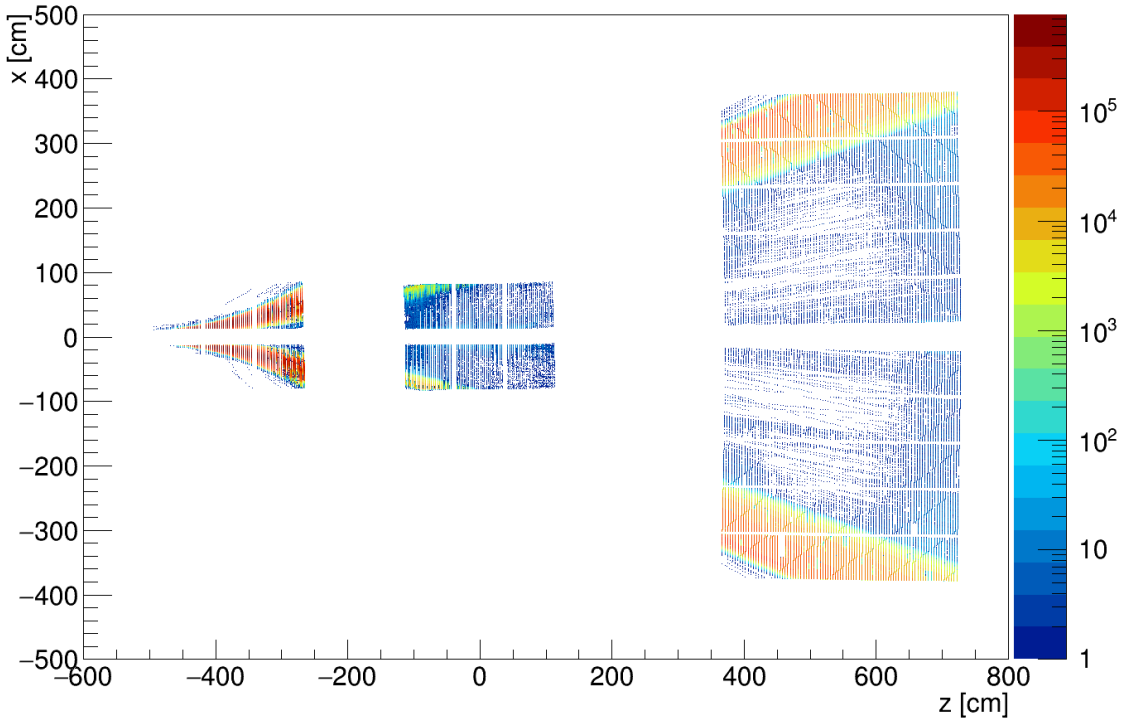

Different ratio cuts

Standard ratio cut

$$0.5 < \frac{\text{clusters}}{\text{potential points}} < 1.1$$

for all TPCs simultaneously.

New ratio cut

Standart ratio cut only for VTPC1 for tracks that fulfill this condition:

pp[VTPC1] > 0 && pp[MTPC] > 0 && clusters[MTPC] == 0 && clusters[VTPC1] >= 15 && pp[VTPC2] <= 24.

Standard ratio cut for all TPCs simultaneously for other tracks.
(pp – potential points)

Different ratio cuts

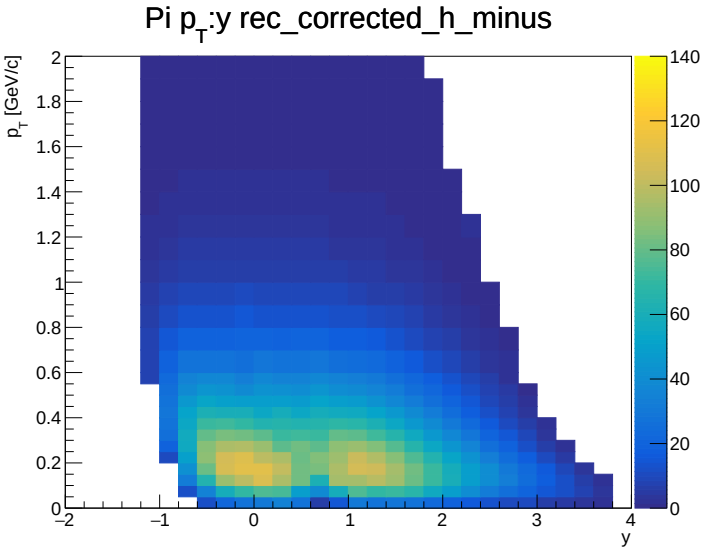

Standard ratio cut

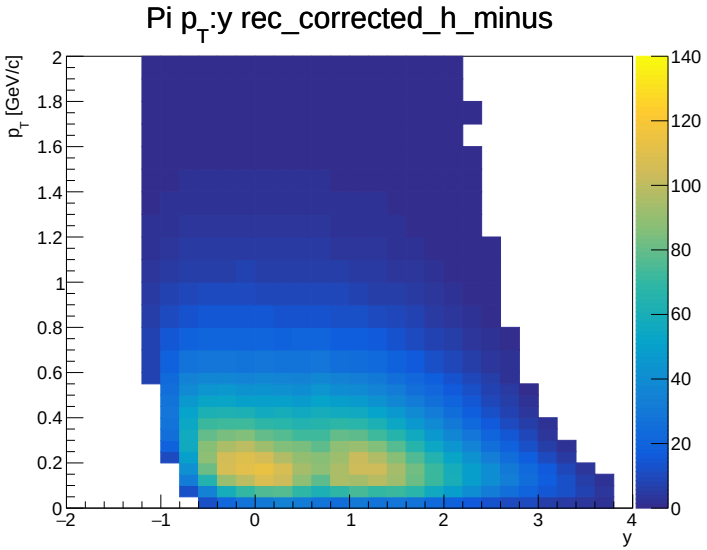

New ratio cut

dN/dy

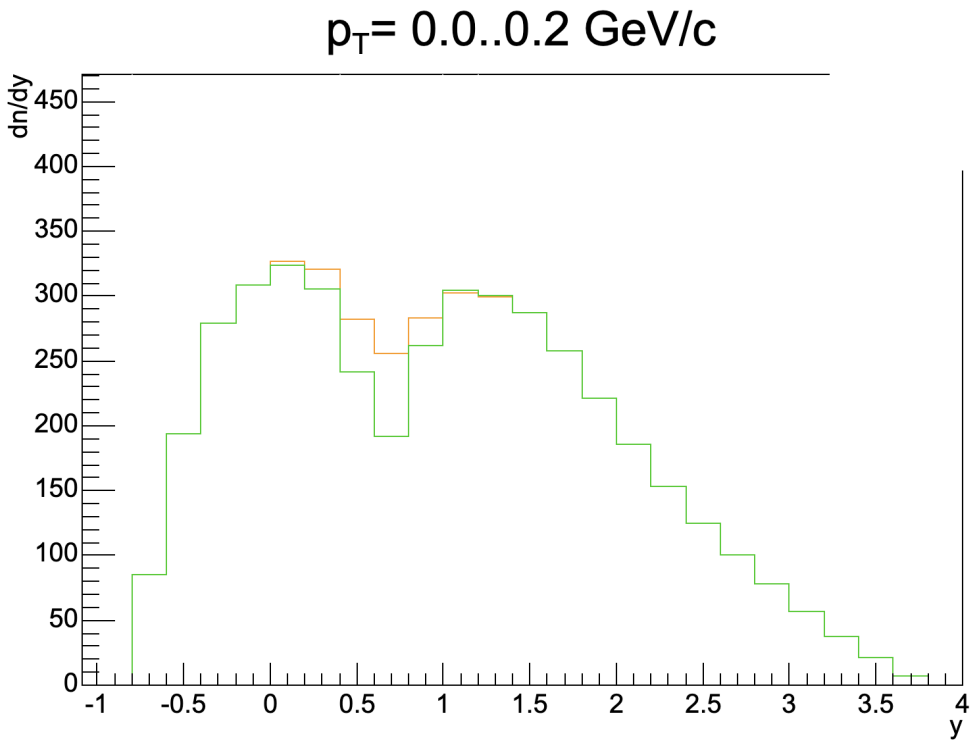

green – old ratio cut, orange – new ratio cut

Summary

Xe+La collisions at 150A GeV/c were analysed.

- Raw spectra of charged hadrons were obtained.
- First corrected spectra of charged hadrons using $\mathrm{d}E/\mathrm{d}x$ method were obtained.
- First corrected spectra of π^- using h^- method were obtained. Problem with the "hole" in the corrected spectra exists. Possible reasons for the "hole":
  - Bad resolution of tracks due to high track density.
  - Split tracks due to inefficient merging (especially for the edges of TPCs).
- Cluster cuts dependence for h^- was studied.
- φ dependence for $\mathrm{d}E/\mathrm{d}x$ was studied, selected range $\varphi \in (-30°, 30°)$.

Further plans

- Detailed studies of the centrality selection using PSD.
- Solving the problem with the “hole”.
- Tuning of MC corrections (feed-down corrections).
- Obtaining final results with statistical and systematic uncertainties.
- Analysis of other energies ($13A$ – $75A$ GeV/c).

Final results will allow to study system size dependence better and add new points to “kink”, “horn” and “step” plots.

Backup Slides

Horn as a signature of the onset of deconfinement

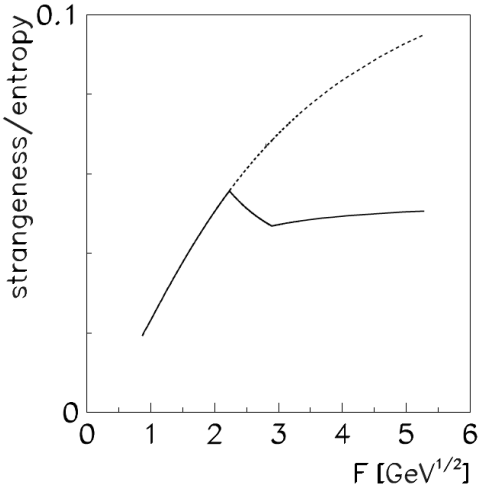

What is strangeness?

- Strangeness is a property of particle expressed as a quantum number.
- Total strangeness of particle: $S = -(n_s - n_{\bar{s}})$,
  n_s – number of strange quarks,
  $n_{\bar{s}}$ – number of strange antiquarks.
- Net strangeness of the system: $\sum_i S_i$.

- Net strangeness is conserved in all interactions except weak.
- We measure only **primary particles** – created in strong and EM interactions.
- No strange content in colliding nuclei.

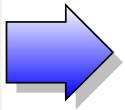

In heavy ion collision **total net strangeness is 0**.

In HIC strangeness is defined as a **number of $s\bar{s}$ pairs** ($N_{s\bar{s}}$).

Distribution of strangeness between hadrons

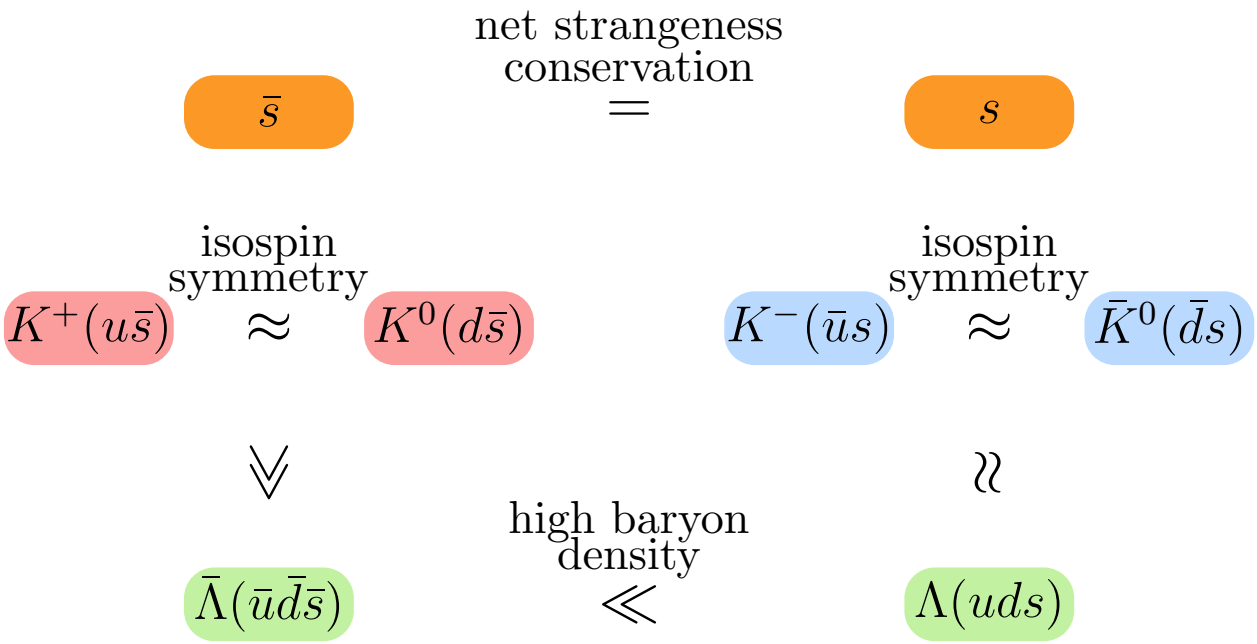

– sensitive to strangeness content only

– sensitive to strangeness content and baryon density

How to measure strangeness

$$2\langle N_{s\bar{s}}\rangle = \langle \Lambda + \bar{\Lambda}\rangle + \langle K^+ + K^- + K^0 + \bar{K}^0\rangle + ...$$

$$2\langle N_{s\bar{s}}\rangle \approx \langle \Lambda\rangle + \langle K^+ + K^- + K^0 + \bar{K}^0\rangle,$$

$$\langle N_{s\bar{s}}\rangle \approx \langle \Lambda\rangle + \langle K^- + \bar{K}^0\rangle \approx \langle K^+ + K^0\rangle \approx 2\langle K^+\rangle.$$

How to measure entropy

Entropy $\sim \langle \pi \rangle$

$$\langle \pi \rangle = \langle \pi^+ + \pi^0 + \pi^- \rangle \approx 3\langle \pi^+ \rangle$$

Experimental measure of strangeness to entropy ratio

$$\frac{\text{strangeness}}{\text{entropy}} \sim \frac{\langle N_{s\bar{s}}\rangle}{\langle \pi \rangle} \approx \frac{2\langle K^+\rangle}{3\langle \pi^+\rangle}$$

Strangeness at phase transition

$$\langle N_i \rangle = \frac{gV}{(2\pi)^3} \int \mathrm{d}^3 p \frac{1}{\exp\left(E/T\right) \pm 1}$$

confined matter

K-mesons

$g_K = 4$

$2M_K \approx 2 \times 500\text{MeV}$

heavy – $M_K > T_c$

Phase transition
$T_c \approx 150\text{MeV}$

quark-gluon plasma

s, $\bar{s}$ - quarks

$g_s = 12$

$2M_s \approx 2 \times 100\text{MeV}$

light – $M_s < T_c$

$$\langle N_K \rangle = g_K V \left(\frac{M_K T}{2\pi}\right)^{\frac{3}{2}} \exp\left(-M_K/T\right)$$

$$\langle N_s \rangle = g_s V \frac{2\pi^2}{4 \cdot 45} \cdot T^3$$

Strangeness production is sensitive to phase transition.

Strangeness/entropy at phase transition

hadron gas

$$\frac{\langle K \rangle}{\langle \pi \rangle} \sim \frac{(M_K T)^{\frac{3}{2}}}{T^3} \exp^{-\frac{M_K}{T}}$$

quark-gluon plasma

$$\frac{\langle s \rangle}{\langle u + d + g \rangle} \sim \frac{T^3}{T^3} = \text{const}(T)$$

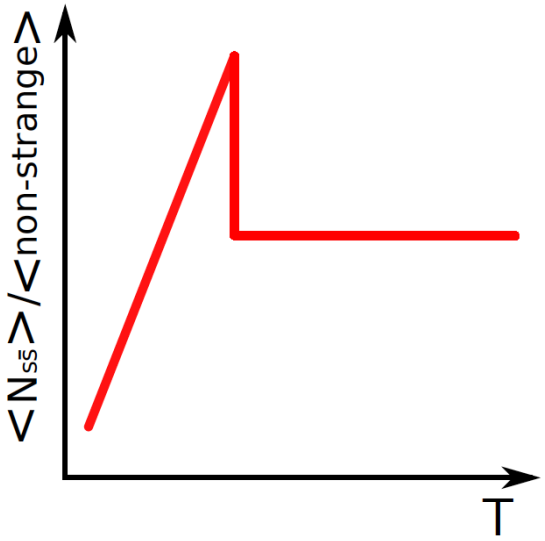

Proton rapidity spectra shape as a signature of the onset of deconfinement

dn/dy spectra of protons

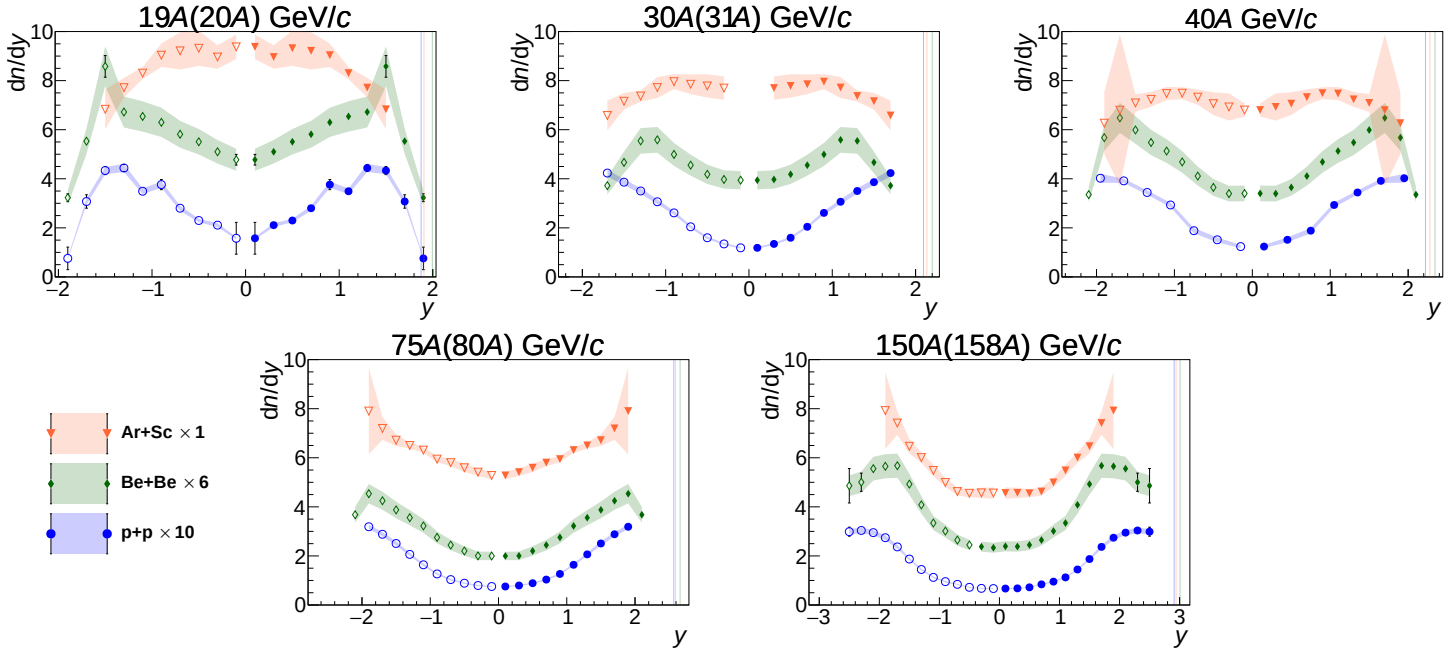

"Dip" for p+p and Be+Be. "Peak-dip" transition for Ar+Sc.

p+p: NA61/SHINE, EPJ C 77 (2017) 671
Be+Be: NA61/SHINE, EPJ C 80 (2020) 961
Ar+Sc: NA61/SHINE preliminary

dn/dy spectra of protons

Two classes of collisions:

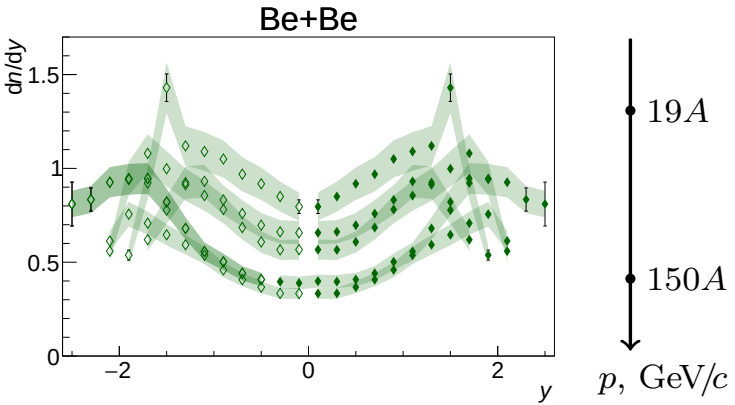

"Dip" for small systems: p+p and Be+Be

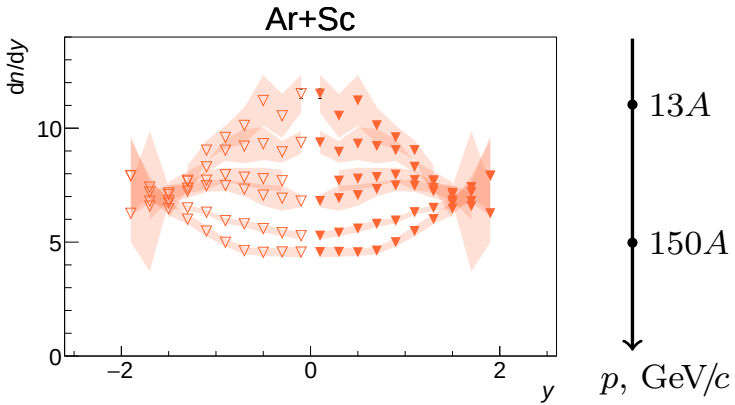

"Peak-dip" transition for medium size system: Ar+Sc

Comparison of NA61/SHINE data with Pb+Pb world data

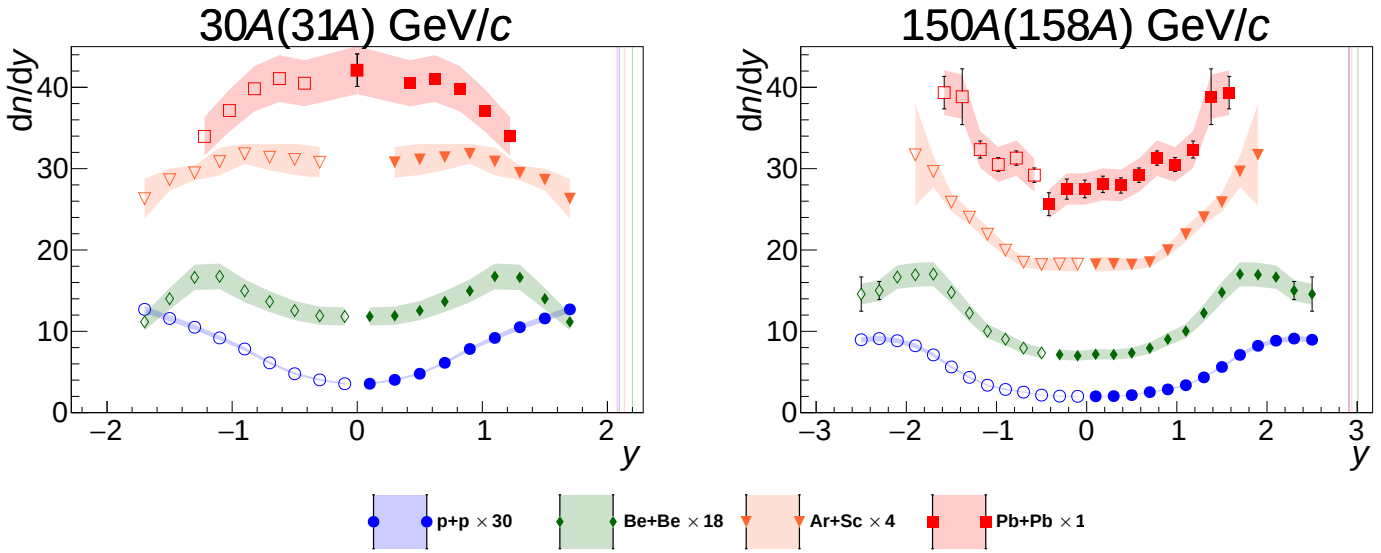

- "Peak-dip" transition is observed medium and heavy systems: Ar+Sc and Pb+Pb within SPS energy range.
- No such transition for small systems: p+p and Be+Be.

Pb+Pb at 30A GeV/c: NA49 preliminary
Pb+Pb at 150A GeV/c: NA49, PRC 83 (2011) 014901

System size and energy dependance of the shape of proton dn/dy spectra

p, GeV/c	$\sqrt{s_{NN}}$, GeV	p+p	Be+Be	Ar+Sc	Pb+Pb
13A (10.5A)	5.1	–	–	peak	flat?
20A (19A)	6.3	dip	dip	flat?	flat?
31A (30A)	7.7	dip	dip	flat?	peak
40A	8.8	dip	dip	flat?	dip
80A (75A)	12.3	dip	dip	dip	dip
158A (150A)	17.3	dip	dip	dip	dip

- "Peak-dip" transition is observed medium and heavy systems: Ar+Sc and Pb+Pb within SPS energy range.
- No such transition for small systems: p+p and Be+Be.

$\mathrm{d}E/\mathrm{d}x$ method for the identification of charged particles

How does TPC work?

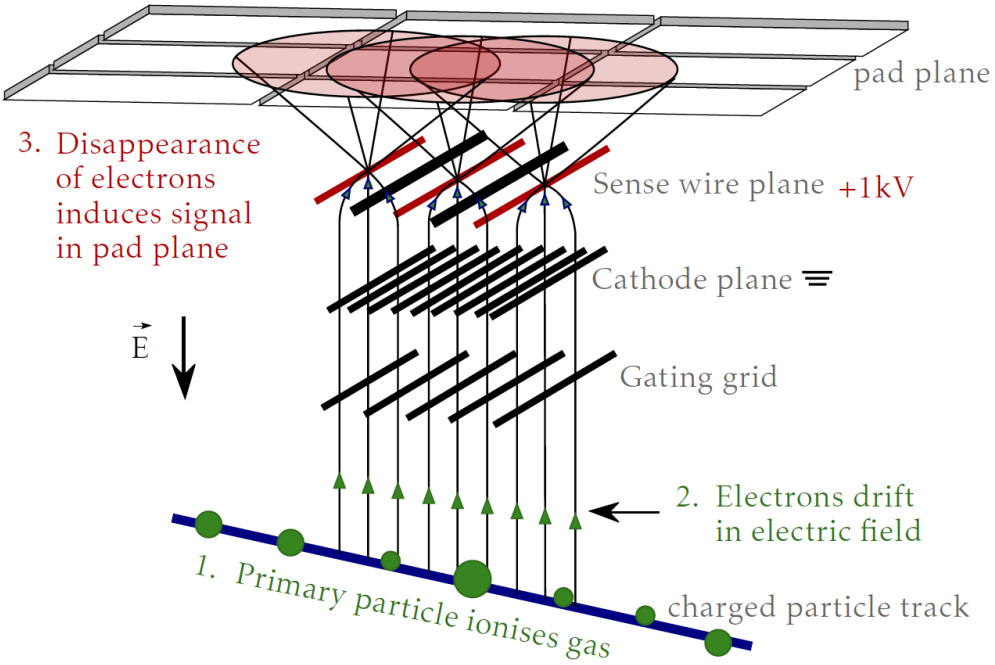

Right side tracks

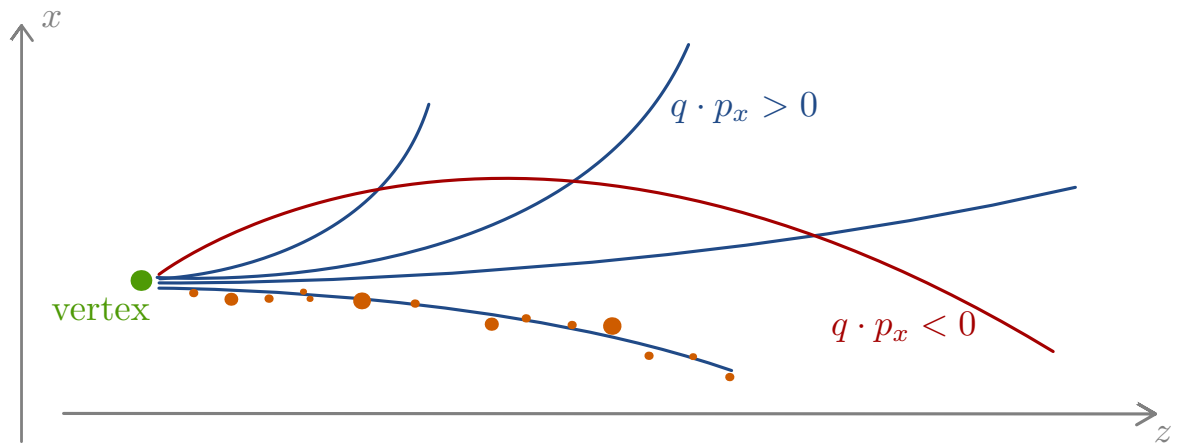

Tracks with $q \cdot p_x > 0$ are named Right side tracks (RSTracks).

$\langle dE/dx \rangle$ as a function of $\beta\gamma = p/Mc$

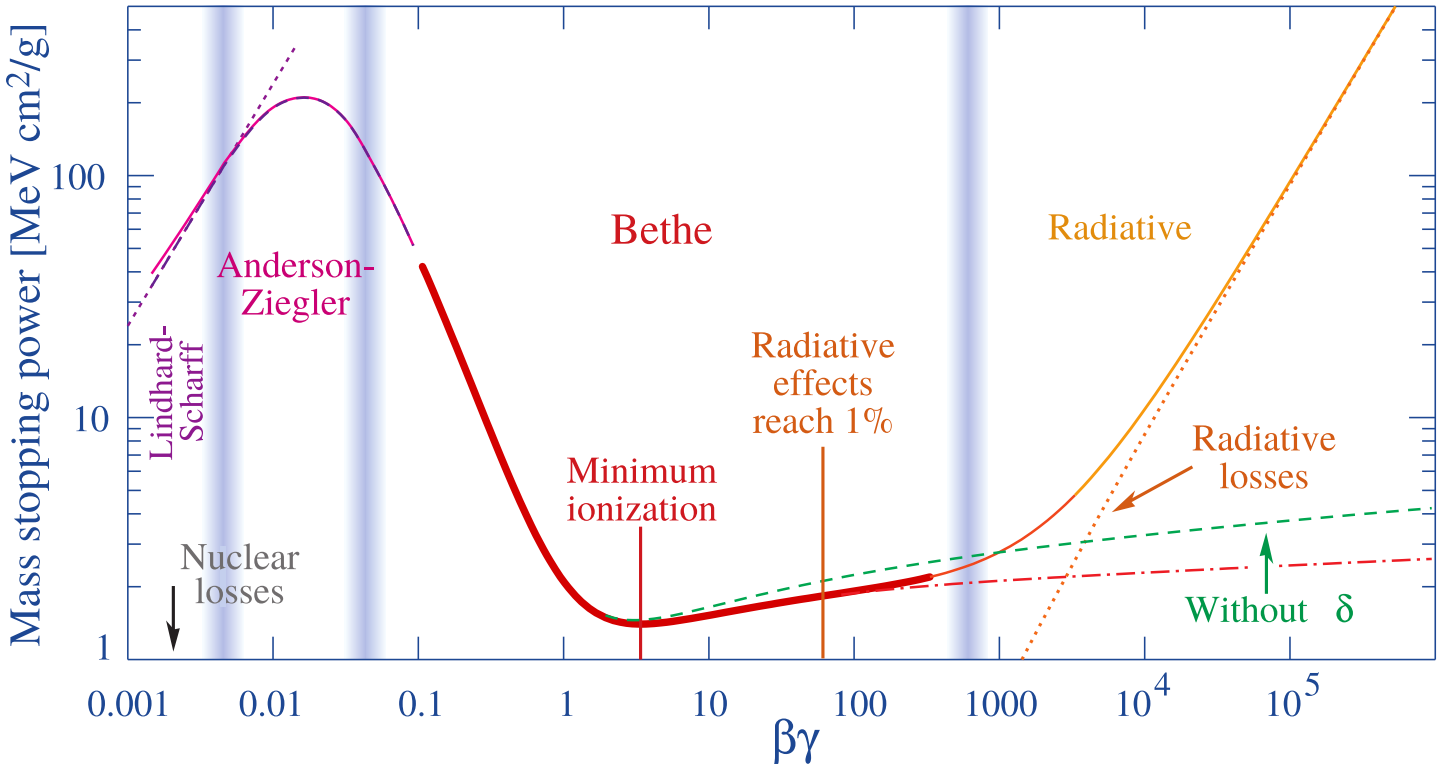

Bethe: $\left\langle -\frac{dE}{dx} \right\rangle = \frac{A}{\beta^2} \left[\ln B\beta^2\gamma^2 - 2\beta^2 - \delta(\beta\gamma) \right], \; (0.1 \leq \beta\gamma \leq 1000)$

$\mathrm{d}E/\mathrm{d}x$ vs p after Track status cut

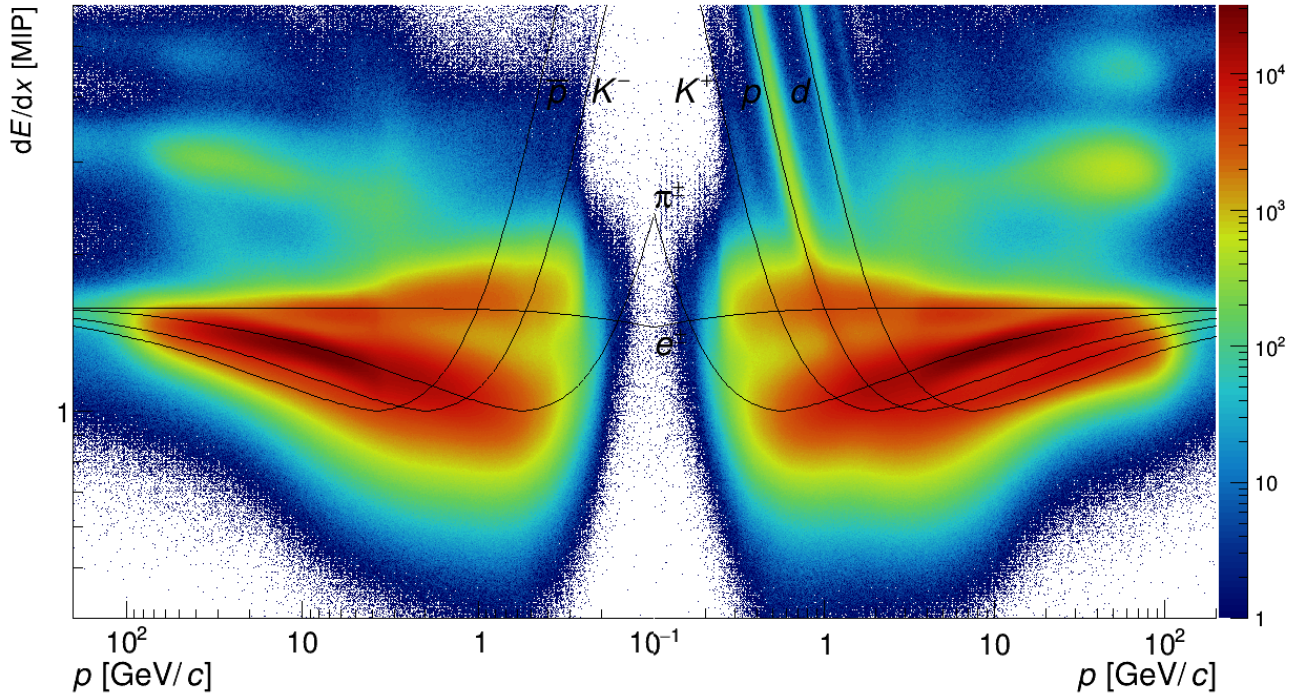

$\mathrm{d}E/\mathrm{d}x$ vs p after all cuts

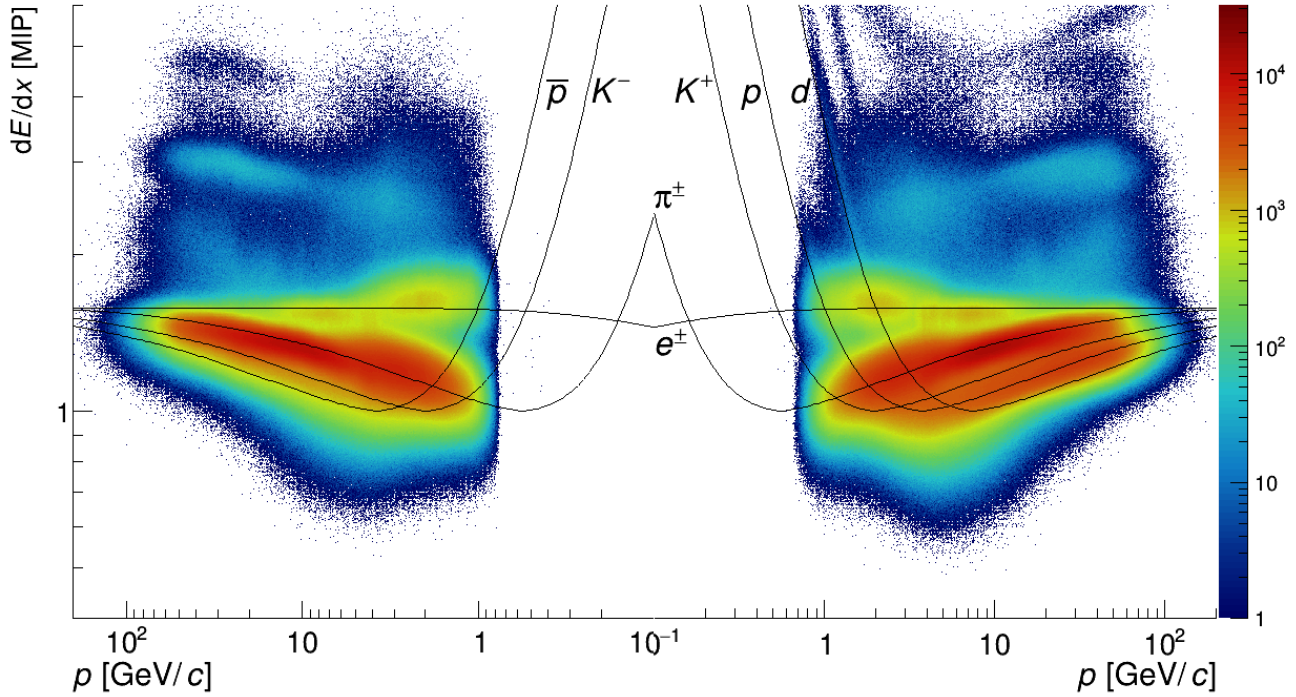

Parameters of fit for 25.12_31.62_0.45_0.50 histograms:

- σ_0, δ_0, σ_e, δ_e, α,
- π peak position,
- e peak position,
- p/π, K/π, d/π peak positions,
- N_π, N_K, N_p, N_d, N_e.

- red – fixed parameters,
- green – parameters different for $-$ and $+$ histograms,
- black – parameters common for $-$ and $+$ histograms.

Total number of Free parameters:
20 for both histograms (NFree),
13 for one histogram (NFree_1).

Azimuthal angle φ

Why do we have φ dependence?

- **Geometry of the detector** – track length is bigger for the middle of the detector, drift length is smaller fot the top of the detector.
- Calibration and calculation of dE/dx – **drift of** dE/dx **with** y (vertical coordinate).

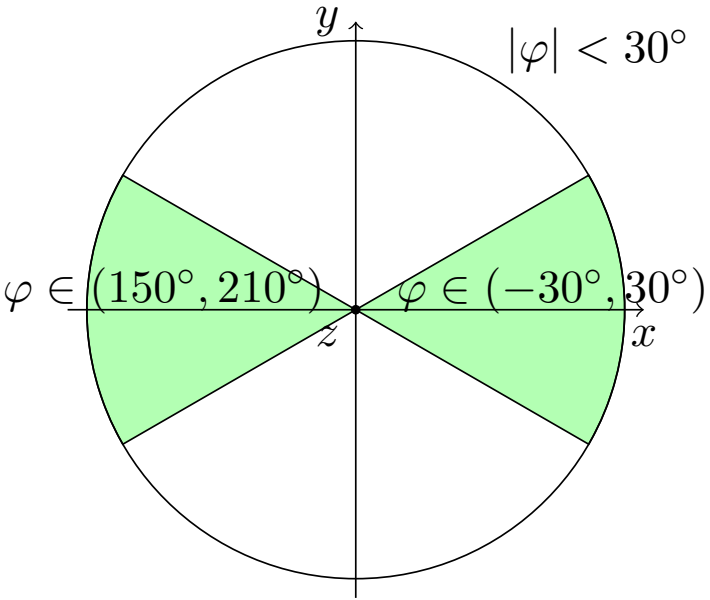

Consequences of φ cut

\+ Possibly smaller systematic uncertainties (due to removing biases).
− Bigger statistical uncertainties.

$p = 5.01..6.31$ GeV/c, $p_T = 0.25..0.30$ GeV/c

$15° < \varphi < 45°$

worse resolution

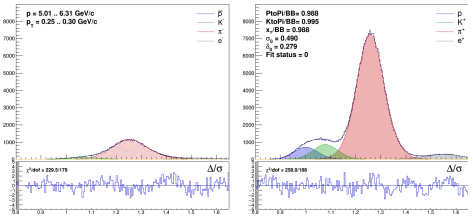

$45° < \varphi < 75°$

worst resolution

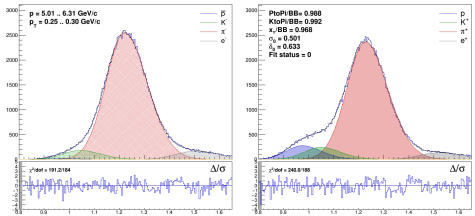

$-15° < \varphi < 15°$

best resolution

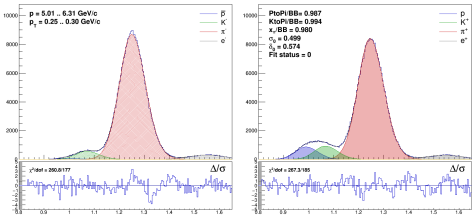

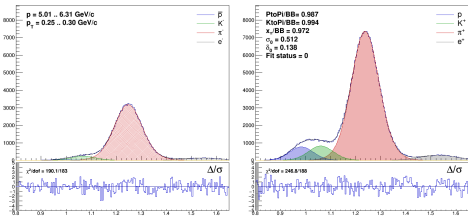

$-45° < \varphi < -15°$

worse resolution

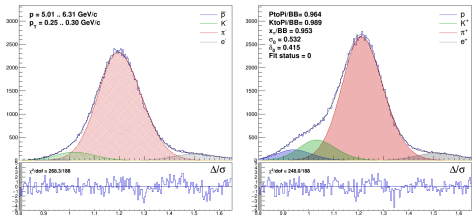

$-75° < \varphi < 45°$

worst resolution

Residuals

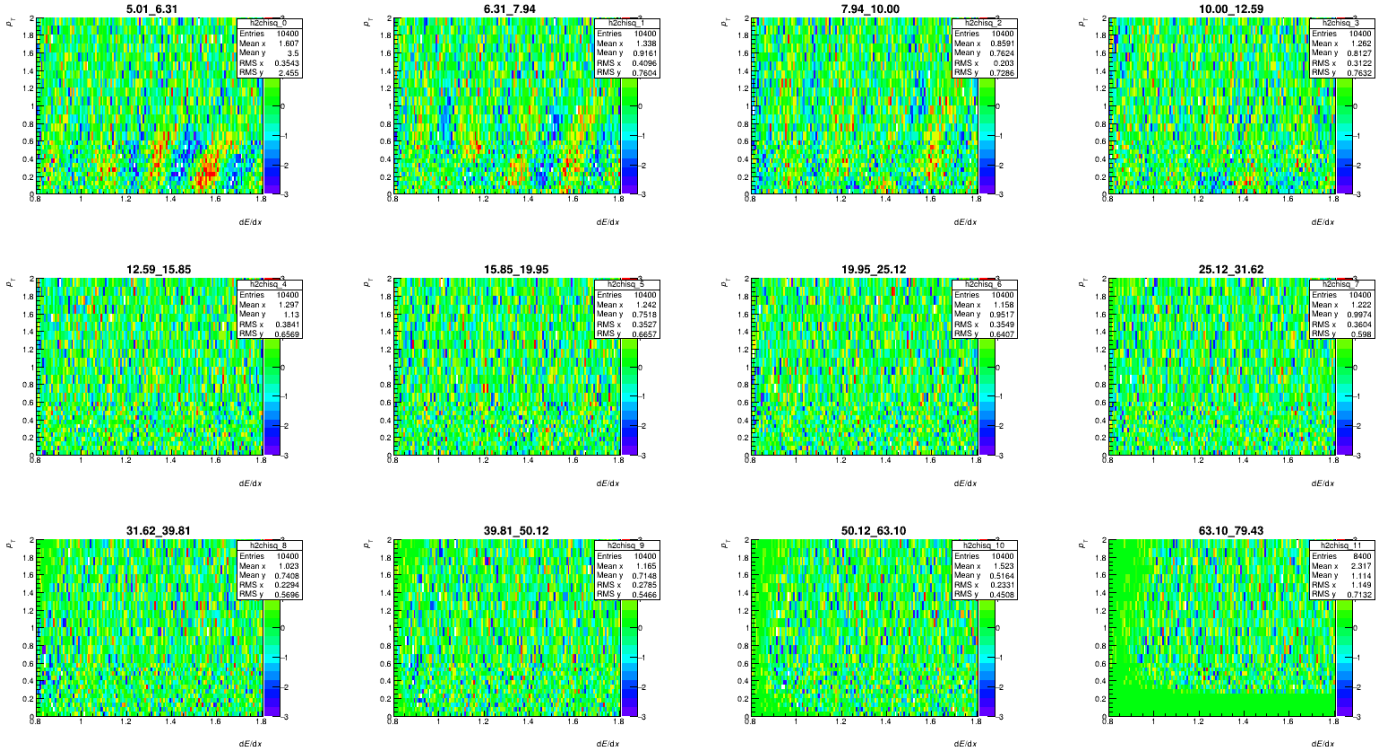

"Waves" for small momenta – imperfect calibration and/or fitted model.

Ratios of particle yield to all particles

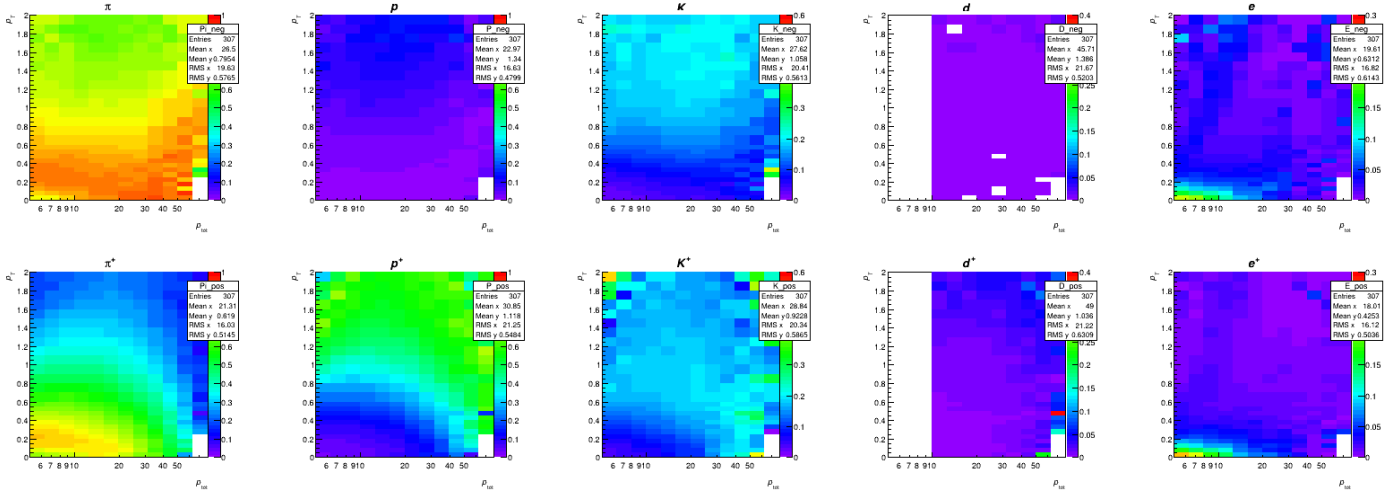

- The transitions are smooth – that's good.
- Fits are stable.

RMS for K peak dependence on $\varphi, \varphi \in (-15°, 15°)$

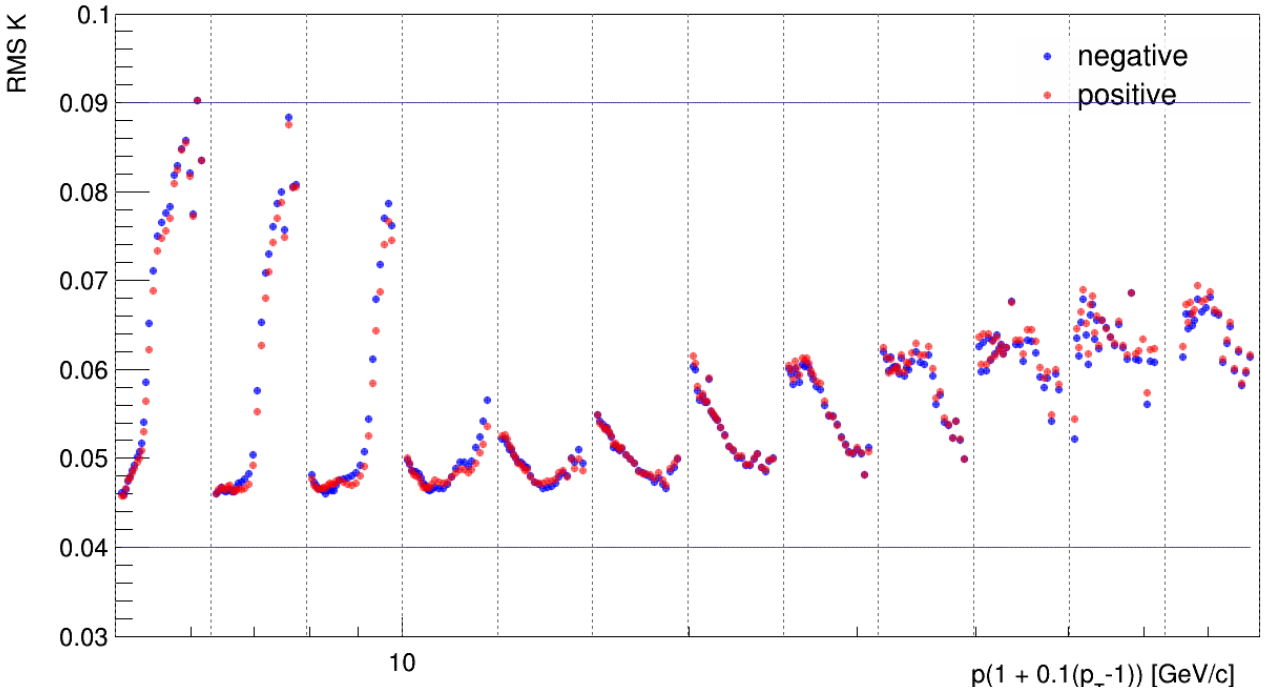

- RMS is anticorrelated with n_{pts}.
- n_{pts} depends on φ.
- Lower RMS results in higher PID resolution, $\rightarrow$ more accurate K yield.

K peak RMS dependence on φ

middle

$-15^\circ < \varphi < 15^\circ$

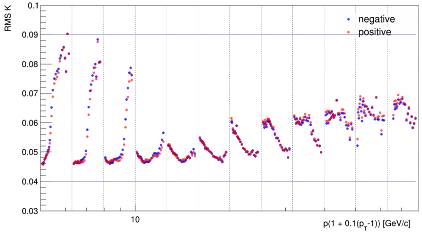

top

$15^\circ < \varphi < 45^\circ$

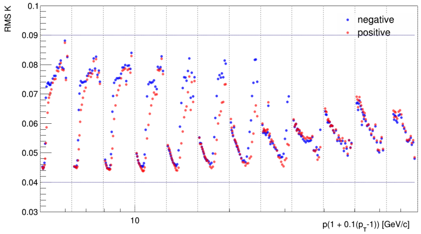

very top

$45^\circ < \varphi < 75^\circ$

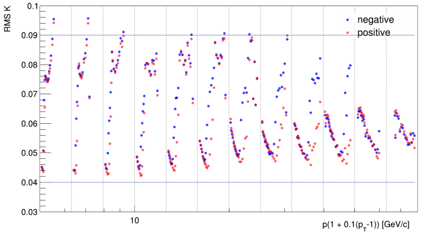

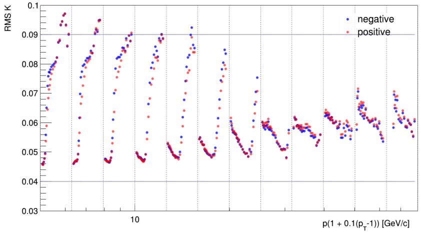

bottom

$-45^\circ < \varphi < -15^\circ$

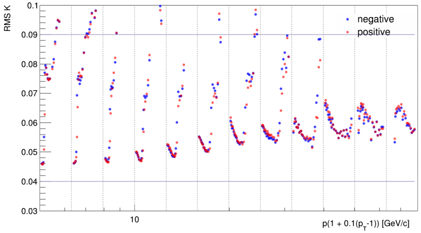

very bottom

$-75^\circ < \varphi < -45^\circ$

RMS is smaller for small $|\varphi|$, $\rightarrow$ we should choose small $|\varphi|$ range.

RMS for K

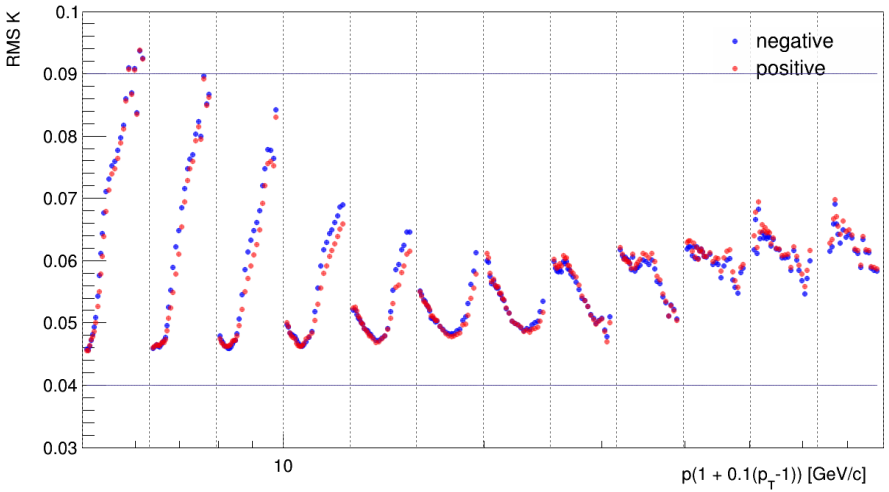

← Xe+La

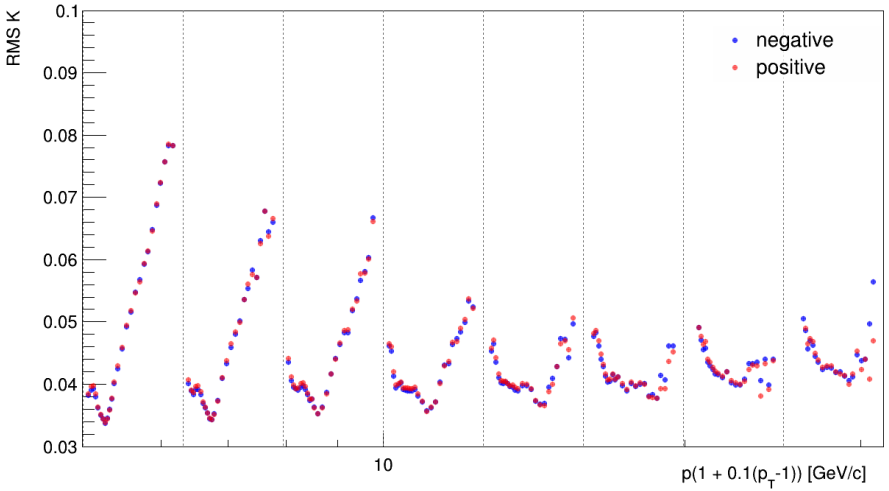

← Ar+Sc

p to K peak distance to K peak RMS dependence on φ

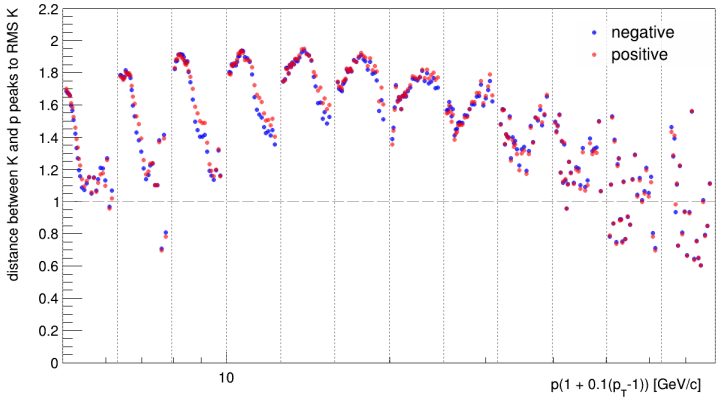

$-30^\circ < \varphi < 30^\circ$

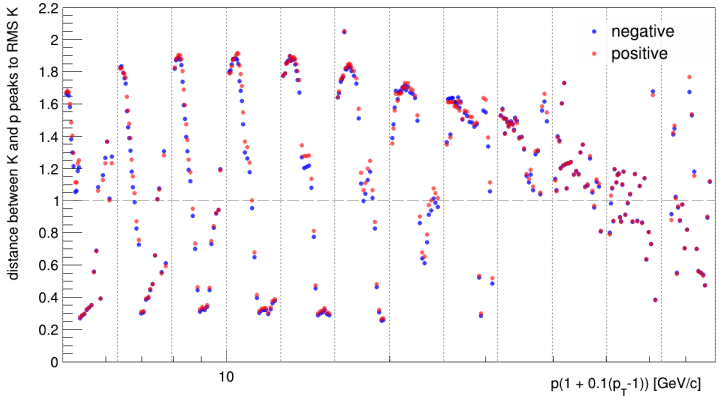

all φ

p to K peak distance to RMS is bigger for $\varphi \in (-30^\circ, 30^\circ)$, $\rightarrow$ we choose $\varphi \in (-30^\circ, 30^\circ)$.

σ_0 dependence on φ

middle
$-15° < \varphi < 15°$

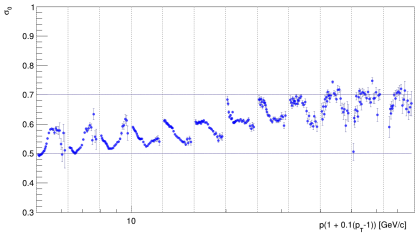

top
$15° < \varphi < 45°$

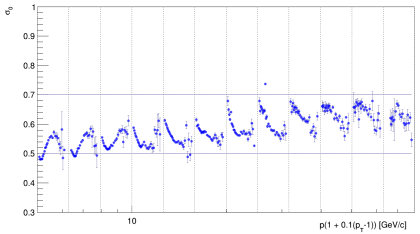

very top
$45° < \varphi < 75°$

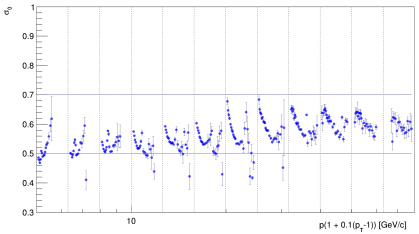

bottom
$-45° < \varphi < -15°$

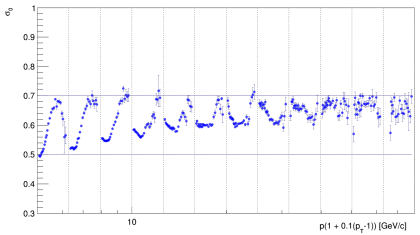

very bottom
$-75° < \varphi < -45°$

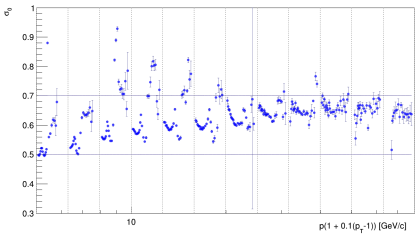

σ_0 is undependent on n_{pts}.

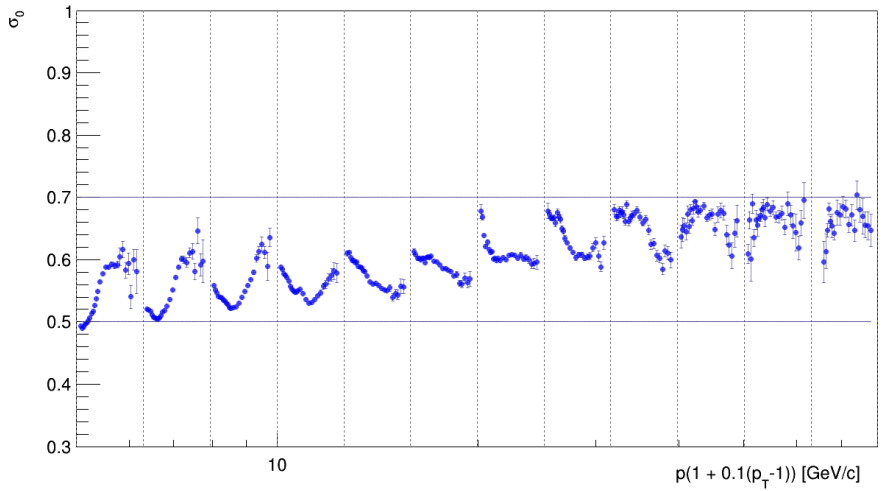

σ_0

$\leftarrow$ Xe+La

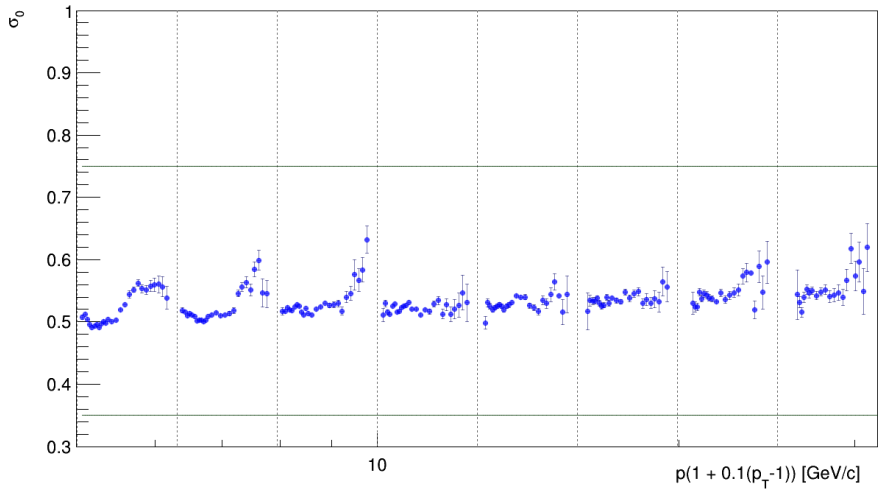

$\leftarrow$ Ar+Sc

π peak position dependence on φ

middle

$-15° < \varphi < 15°$

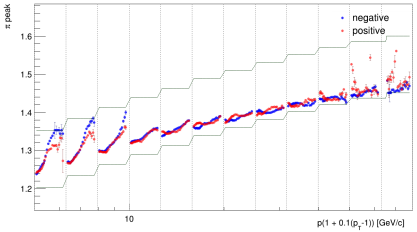

top

$15° < \varphi < 45°$

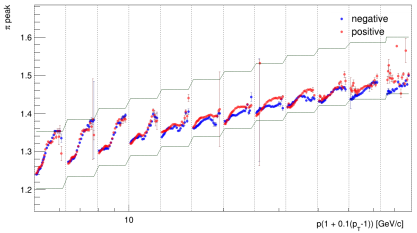

very top

$45° < \varphi < 75°$

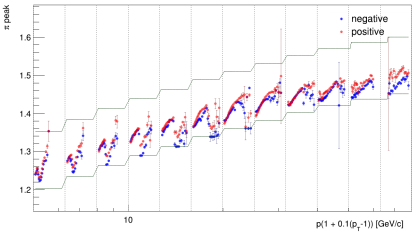

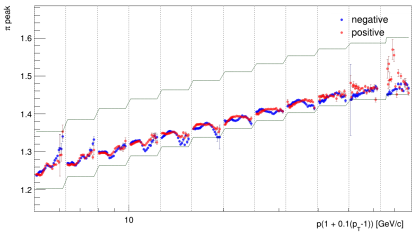

bottom

$-45° < \varphi < -15°$

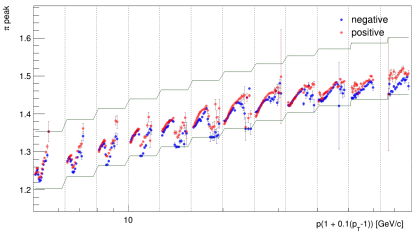

very bottom

$-75° < \varphi < -45°$

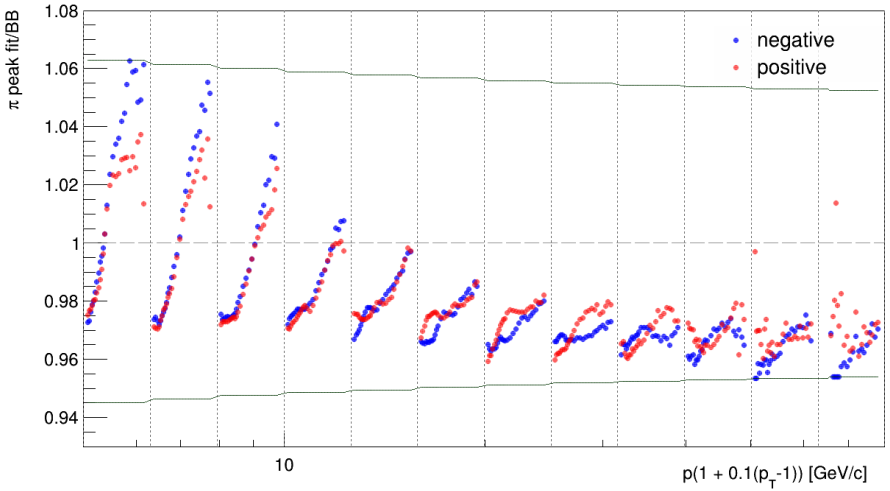

π/BB

$\leftarrow$ Xe+La

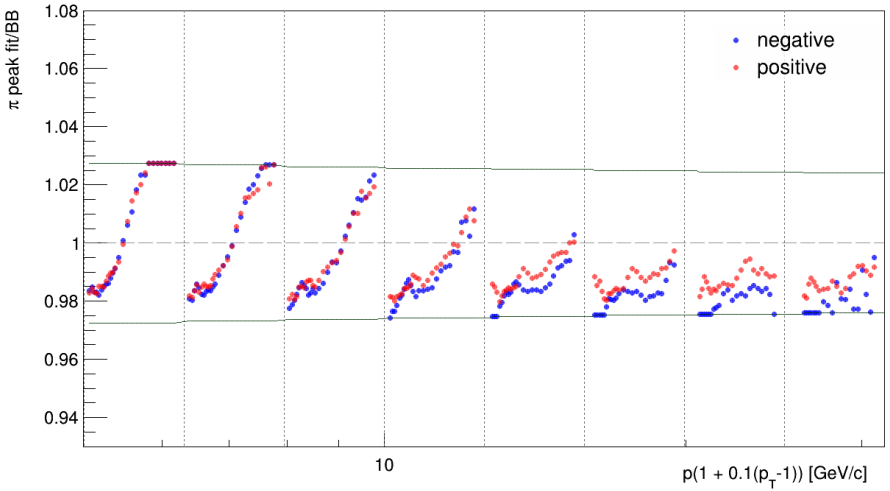

$\leftarrow$ Ar+Sc

$p = 7.94..10.00$ GeV/c, $p_T = 0.40..0.45$ GeV/c

$15° < \varphi < 45°$

$45° < \varphi < 75°$

$-15° < \varphi < 15°$

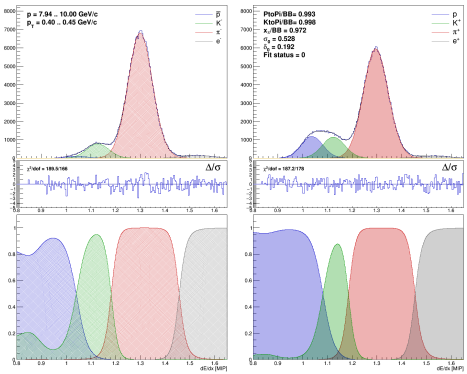

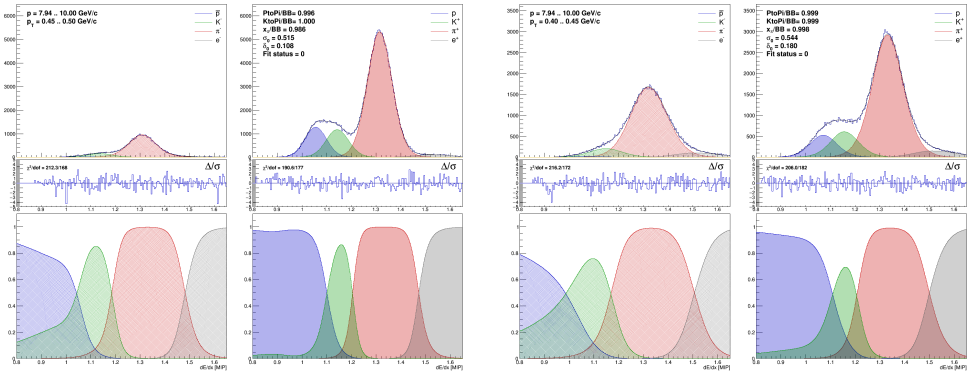

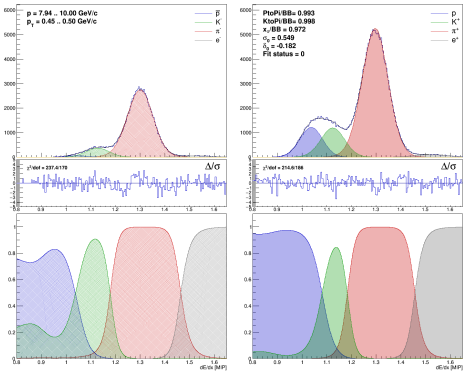

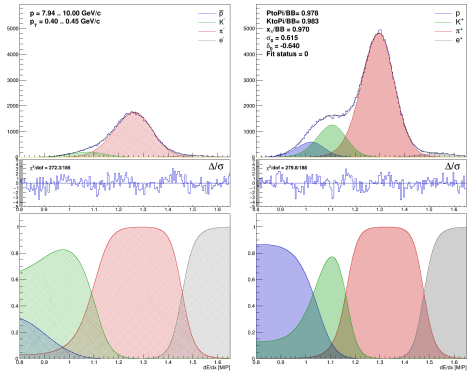

$-45° < \varphi < -15°$

$-75° < \varphi < 45°$

Identity method with interpolation

Interpolation in p:

$$W = W^0 + \frac{\log p - \log p^0}{\log p' - \log p^0} \cdot (W' - W^0),$$

Interpolation in p_T:

$$W = W^0 + \frac{p_T - p_T^0}{p_T' - p_T^0} \cdot (W' - W^0),$$

p^0, p_T^0 – center of the bin,
p' – center of the closest p-bin,
p_T' – center of the closest p_T-bin.

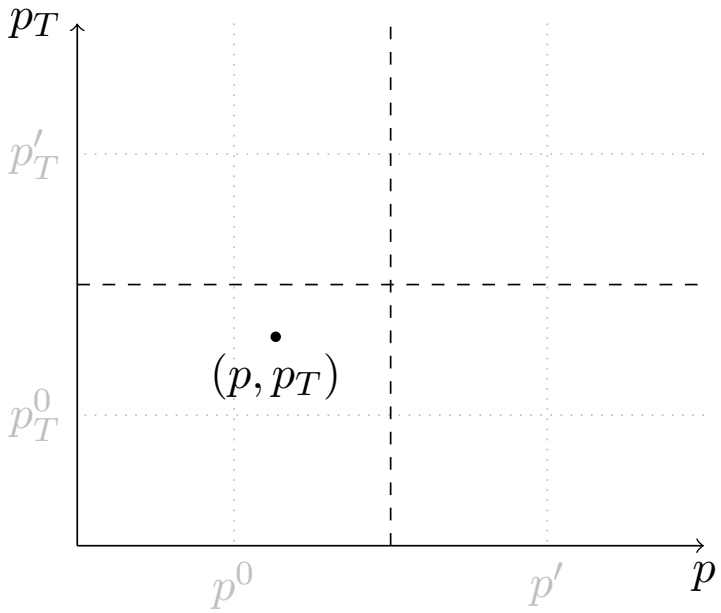

MC corrections

- $N_{\text{MC events}} = 100000$ (more events will be available soon),
- Current corrections:

$$n_i^{\text{corrected}} = n_i^{\text{raw data}} \times \frac{n_i^{\text{MCgen}}}{n_i^{\text{MCrec}}},$$

- Planned corrections:

$$n_i^{\text{corrected}} = (n_i^{\text{raw data}} - n_i^{\text{MCrec decay}}) \times \frac{n_i^{\text{MCgen}}}{n_i^{\text{MCrec primary}}}.$$

- $n_i^{\text{MCrec decay}}$ will be tuned to account for MC model inaccuracy of strange particle yields.

MC correction factors (first try)

Negative:

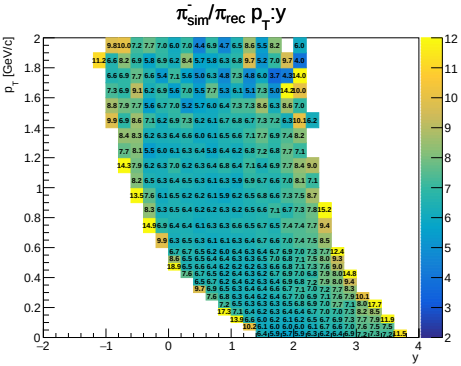

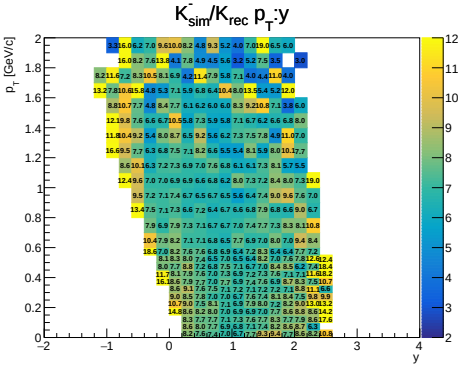

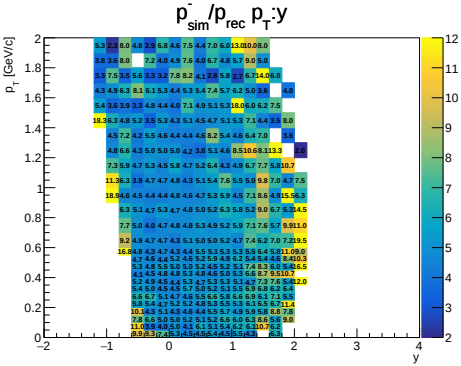

Positive:

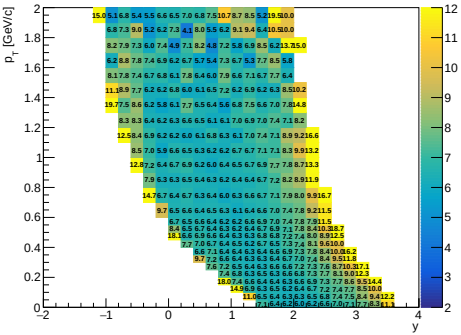

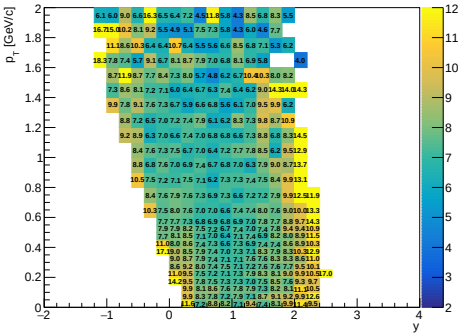

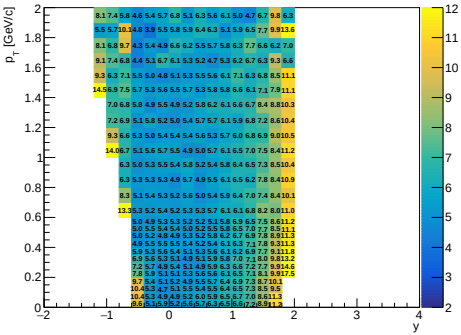

Data selection: Event cuts

Two types of cuts:

- upstream (blue) – select events with well defined beam particle (not biasing),
- downstream (red) – select good measured central events (may be biasing).

	Events	After cut / All events
Before cuts:	4737271	
After T2 cut:	3706646	0.78
After WFA cut:	3300528	0.70
After Good BPD cut:	3298225	0.70
Has Main and Primary vertex:	3297591	0.70
Perfect Fit of momentum:	3259094	0.69
Good Z Position:	3126078	0.66

Data selection: Vertex track cuts

To select well measured charged particle tracks.

	Tracks	After cut / After Track status cut
Before cuts:	22838147516	
After Track status cut:	1743554747	1
VTPC clusters > 15:	1307284896	0.75
All clusters > 30:	902007423	0.52
Ratio cut:	811076867	0.47
$b_x < 4$ cm, $b_y < 2$ cm:	793820413	0.46
RSTracks:	463053931	0.27
$\lvert\varphi\rvert < 30^\circ$ (only for $\mathrm{d}E/\mathrm{d}x$):	167770312	0.10

Clusters distributions. $y = 0.4 - 0.8$, $p_T = 0.1 - 0.3$

VTPC1 clusters

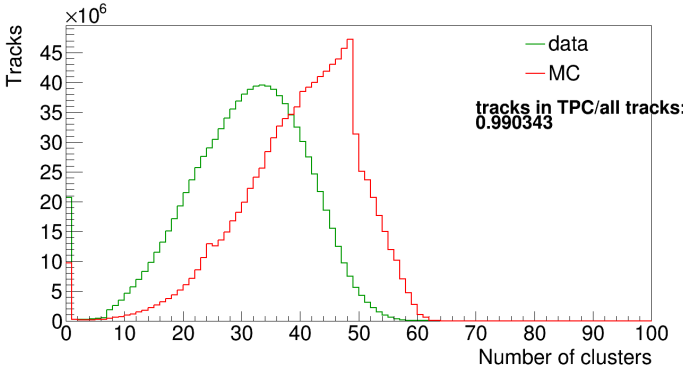

VTPC2 clusters

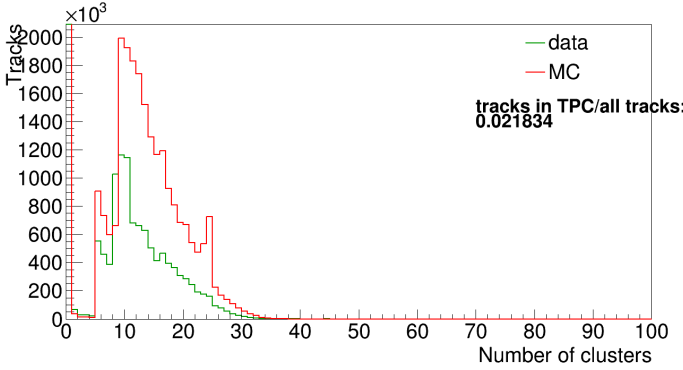

Vertex track cuts:
Track status, Impact parameter, RSTracks, All clusters > 5

MTPC clusters

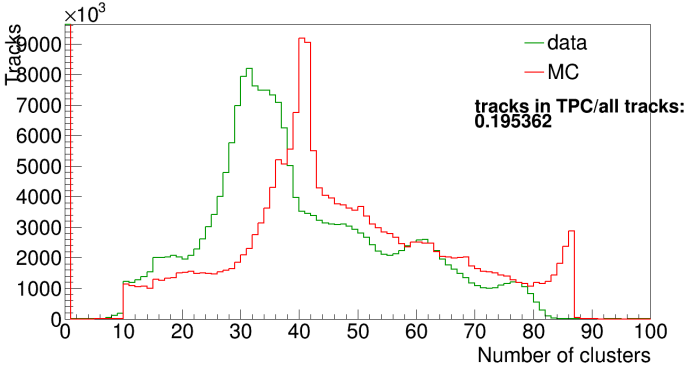

Data distributions are shifted and smeared comparing to MC. Also, they are shifted comparing to the distributions of all tracks.